Title
Folding amphipathic helices into membranes: Amphiphilicity trumps hydrophobicity

Journal
Journal of Molecular Biology, 370(3)

ISSN
0022-2836

Authors
Fernández-Vidal, Mónica
Jayasinghe, Sajith
Ladokhin, Alexey S
et al.

Publication Date
2007-07-01

Peer reviewed

FOLDING AMPHIPATHIC HELICES INTO MEMBRANES: AMPHIPHILICITY TRUMPS HYDROPHOBICITY

Mónica Fernández-Vidal[1,4], Sajith Jayasinghe[2], Alexey S. Ladokhin[3], and Stephen H. White[1]

[1]Department of Physiology and Biophysics, University of California at Irvine, Irvine, CA 92697-4560, USA. [2]Department of Chemistry and Biochemistry, California State University at San Marcos, San Marcos, CA 92096, USA. [3]Department of Biochemistry and Molecular Biology, University of Kansas Medical Center, Kansas City, KS 66160-7421, USA. [4]Present address: Dept. of Peptide and Protein Chemistry, IIQAB-CSIC, 08034 Barcelona, Spain. Correspondence should be addressed to S.H.W. (stephen.white@uci.edu) or A.S.L. (aladokhin@kumc.edu).

Running Title: Amphipathic Helix folding

Key Words: antimicrobial peptides, toxins, membrane proteins, peptide secondary structure, hydrophobic moment

ABSTRACT

High amphiphilicity is a hallmark of interfacial helices in membrane proteins and membrane-active peptides, such as toxins and antimicrobial peptides. Although there is general agreement that amphiphilicity is important for membrane-interface binding, an unanswered question is its importance relative to simple hydrophobicity-driven partitioning. We have examined this fundamental question using measurements of the interfacial partitioning of a family of seventeen-residue amidated-acetylated peptides into both neutral and anionic lipid vesicles. Composed only of Ala, Leu, and Gln residues, the amino acid sequences of the peptides were varied to change peptide amphiphilicity without changing total hydrophobicity. We found that peptide helicity in water and interface increased linearly with hydrophobic moment, as did the favorable peptide partitioning free energy. This observation provides simple tools for designing amphipathic helical peptides. Finally, our results show that helical amphiphilicity is far more important for interfacial binding than simple hydrophobicity.

The amphipathic (or amphiphilic) helix is an important structural motif in proteins. Its most common representation shows polar residues along the length of one-half of a helix surface and non-polar residues along the opposite surface (Figure 1). This polar-nonpolar asymmetry, characterized mathematically by the so-called hydrophobic moment[1] (μ_H), makes the amphipathic helix ideally suited for binding to membrane interfaces with the polar surface facing the aqueous phase and the less polar surface facing the membrane interior. This arrangement is often seen in membrane proteins[2,3] where amphipathic helices apparently provide structural stability. But they are also important functionally. For example, amphipathic helices play important functional roles in both ligand-gated[4] (Figure 1) and voltage-gated K^+ channels[5] and in the insertion of disulfide bonds into *Escherichia coli* periplasmic proteins by the DsbB-DsbA complex[6]. Because of its tendency to partition into membrane interfaces (Figure 1) and subsequently permeabilize membranes, the amphipathic helix is a common starting motif for designing or re-engineering antimicrobial peptides[7-12]. Helix amphiphilicity has been widely examined in the context of membrane permeabilization, but little attention has been paid to the relationships between μ_H, peptide helix-forming ability, and membrane affinity. We present here the results of a systematic investigation of the influence of μ_H on the folding and partitioning of membrane-active peptides. We show that μ_H is a far more potent driving force for interfacial partitioning than total peptide hydrophobicity.

Most membrane-active helix-forming peptides have low or moderate helicity in aqueous solution but become highly helical when partitioned into membranes. This is due in part to the potent ability of membranes to promote secondary structure[13-16], a process conveniently described as partitioning-folding coupling[17,18]. A classic example is the partitioning of melittin, a 26-residue peptide that is the principal component of bee venom[19]. Largely unstructured when free in solution, melittin strongly adopts an amphipathic α-helical conformation when partitioned into membranes[20-23]. An important driving force for folding arises from the lower energetic cost of partitioning H-bonded peptide bonds compared to free peptide bonds[17,18,23]. Knowledge of the energetics of this folding process is important for improving the activity of antimicrobial peptides and for understanding the folding and stability of membrane proteins. An essential element of these energetics is the per-residue reduction in free energy, $\Delta G_{residue}$, that drives secondary structure formation in the membrane interface. This parameter, as we shall show, plays a critical role in the development of an analytical description of peptide folding.

Reported values for $\Delta G_{residue}$ for α-helical peptides range between –0.1 and –0.4 kcal mol^{-1} per residue. Ladokhin and White[23] estimated that $\Delta G_{residue}$ = –0.41(±0.06) kcal mol^{-1} for melittin partitioning-folding in zwitterionic large unilamellar vesicles (LUV) by measuring the partitioning free energies and helicities of native melittin and of a diastereomeric analog with four D-amino acids (D4, L-melittin)[24]. At about the same time, Seelig and co-workers[25], using a variant of the native/diastereomeric approach, measured the partitioning of the antimicrobial peptide magainin into small unilamellar vesicles (SUV) formed from POPC and anionic palmitoyloleoylphosphatidylglycerol (POPG). They reported a value of only –0.14 kcal mol^{-1} per residue for $\Delta G_{residue}$. Subsequently, Li *et al.*[26] published a value of –0.25(±0.05) kcal mol^{-1} per residue, using model host-guest fusion peptides. We show here that such differences in $\Delta G_{residue}$ can arise in part from differences in μ_H.

Helical peptides are typically rendered amphipathic by using combinations of charged and hydrophobic residues[27]. But for the experiments reported here, we wished to avoid charged residues because of the non-additivity of Coulombic and hydrophobic interactions[28], and because we wished to examine whether μ_H effects are affected by surface charge. We therefore used electrically neutral peptides whose designs were inspired by the peptides that Baldwin and colleagues used for studies of α-helix stability in aqueous phases[29]. As we describe below, we synthesized a family of peptides of the general form Ac-$A_8Q_3L_4$-GW-NH_2 in which we varied the $A_8Q_3L_4$ sequence to cover a range of μ_H values. The result was a family of peptides with identical hydrophobicities but different hydrophobic moments. We report below each peptide's helicity and folding free energy in buffer and in POPC and POPC:POPG LUV. We show that peptide helicity in water and interface increase linearly with μ_H, as does the magnitude of peptide partitioning free energy.

RESULTS

Thermodynamic Framework

Algorithms for predicting peptide folding and binding to membrane interfaces require an experimentally accessible thermodynamic cycle for analyzing partitioning-folding data[30,31] that yields $\Delta G_{residue}$. Figure 2A shows the thermodynamic cycle that forms the quantitative framework for our data. Its important feature is an experimentally definable unfolded reference state in the aqueous phase, which—as discussed below—is critical for predictions. We consider an equilibrium between four

states: unfolded peptide in the aqueous phase (A) and membrane interface (B), partially folded in aqueous phase (C), and folded in the membrane interface (D). As discussed in detail by Hristova and White[32], experimental determination of ΔG_{AB} for the A ⇆ B leg of the cycle is problematic, because partitioning-folding coupling causes a great excess of D relative to B. To circumvent this problem, Hristova and White[32] developed an experiment-based algorithm for predicting the partitioning of unfolded peptides into POPC interfaces. Based upon an experimental extension of the Wimley-White interfacial hydrophobicity scale[17], the Hristova-White algorithm predicts partitioning with high accuracy[28]. Because ΔG_{AB} can be computed accurately, the experiments described below revolve around systematic experimental determinations of ΔG_{AC} and ΔG_{CD}, from which ΔG_{BD} and $\Delta G_{residue}$ follow. We measured peptide helicity, ΔG_{AC}, and ΔG_{CD} for each member of the Ac-$A_8Q_3L_4$-GW-NH_2 peptide family, as described below. ΔG_{AC} was measured using the alcohol titration method of Hirota *et al.*[33,34] and ΔG_{CD} by circular dichroism and fluorescence titration.

The important feature of the thermodynamic cycle is the A ⇆ B equilibrium, which is not accounted for in the traditional thermodynamic analysis of peptide partitioning[23,25,31] (Figure 2b**)**. This latter thermodynamic scheme is a very practical one, because the C and D states (and therefore ΔG_{CD}) are readily accessible by circular dichroism (CD)[23,25] and fluorescence measurements[35]. But there is a problem: The conformation of the peptide in state C depends inherently on its sequence and aqueous environment, often in complex ways[29,36]. The consequence is that each peptide in, say, a host-guest family can have a different extent of folding in the ΔG_{CD} measurement. This can obscure the true per-residue cost of folding, which is an essential element for a successful prediction algorithm. This problem was ameliorated by Ladokhin and White[23] through the use of diastereomeric peptides that cause the peptide to have similar conformations in states C and C'. Despite its incompleteness, the thermodynamic scheme of Figure 2b nevertheless leads to useful algorithms for estimating partitioning and folding.

Peptide Design and Helicity

All of the peptides had an acetylated N-terminus and amidated C-terminus in order to avoid Coulombic interactions with charged lipids. We found that a test "Baldwin" peptide[29], Ac-$(AAQAA)_3$GY-NH_2, partitioned minimally into POPC vesicles with a $\Delta G \leq -2.2$ kcal mol^{-1}. This peptide thus served as a zero-binding baseline for engineering partitioning upward through systematic alterations in sequence using Ala-to-Leu

substitutions. We replaced the tyrosine residue with tryptophan to facilitate measurements of partitioning free energy by fluorescence titration, and to determine peptide concentration from Trp absorbance at 280 nm (ε_{280} = 5600 M^{-1} cm^{-1}). As in the designs of Chakrabartty and Baldwin[29], Trp was segregated from the rest of the peptide by a Gly residue to reduce the contribution of the aromatic chromophore to the far-UV circular dichroism (CD) spectrum[37].

The peptides synthesized in the course of this study are shown in **Table 1**, along with their hydrophobic moments μ_H and their Wimley-White[17] hydrophobicity scale free energies of transfer, computed using the Hristova-White[32] algorithm that is included in the Totalizer module of MPEx (available on-line at http://blanco.biomol.uci.edu/). Only the peptide $A_8Q_3L_4$–4.72 (i.e., μ_H = 4.72) bound significantly to POPC LUV membranes. Therefore, variants of this peptide were synthesized and used for systematic studies of the relationship between μ_H and the free energies of transfer. The Totalizer results indicated that the free energy of partitioning ΔG_{TM} of Ac-$A_8Q_3L_4$-GW-NH_2 into the membrane from water as a transmembrane helix is unfavorable by +3 kcal mol^{-1}. A similar conclusion was reached using the recently determined biological hydrophobicity scale[38] (ΔG_{TM} = +4.6). It is therefore reasonable to assume that all of the peptides partitioned only into the membrane interface.

The CD spectra of the peptides $A_8Q_3L_4$–5.51, $A_8Q_3L_4$–2.86, and $A_8Q_3L_4$–0.55 are shown in Figure 3. The spectra present two minima (≈222 nm and ≈205 nm) and a maximum at ≈190 nm, which correspond to mixtures of helix and random coil. The fractional helix content (f_α) is directly proportional to the mean molar ellipticity at 222 nm ($[\Theta]_{222}$ in units of deg cm^2 $dmol^{-1}$) and was calculated as described in Materials and Methods. As shown in Figure 4, the helical content in buffer (▲) increases linearly with hydrophobic moment, ranging from 9% for the peptide with the lowest μ_H to 40% for the peptide with the maximum μ_H (see Supplementary Table S1 online).

Free Energy of Folding in Buffer: ΔG_{AC}

Because our model peptides were not in a completely unfolded state in water, the free energy difference ΔG_{AC} between the fully unfolded and partially folded states had to be determined. ΔG_{AC} was measured using the alcohol-induced α-helix-formation method of Hirota and colleagues[33,34] using both methanol (data not shown) and trifluoroethanol (TFE) to induce folding. The TFE titration data are included in Supplementary Material (Figs. S1 and S2). Helicity was found to increase with alcohol

concentration, strictly following a Boltzmann distribution, as expected for a two-state transition. Because the TFE titration curves reached saturation, $[\Theta]_{222}$ values could be established for fully unfolded and fully helical peptides. These values allowed determination of the fractions of helical (f_α) and unfolded ($f_u = 1 - f_\alpha$) peptides for a particular TFE concentration to be determined, including [TFE] = 0. Values of f_α for [TFE] = 0 are shown in Supplementary Table S1 online. The free energy change ΔG_0 for folding in the absence of TFE is given by $\Delta G_0 = -RT\ln K_\alpha \equiv \Delta G_{AC}$, where $K_\alpha = f_\alpha/f_u$. The free energies (Supplementary Table S1 online), ranging from +1.32(±0.06) kcal mol^{-1} for $A_8Q_3L_4$–0.55 to +0.27(±0.04) kcal mol^{-1} for $A_8Q_3L_4$–5.54, are plotted in Figure 5.

Interfacial Partitioning of Partially-Folded Peptides: ΔG_{CD}

Partitioning of the peptides into LUV membranes resulted in the formation of α-helical structure. As in aqueous solution (above), the fractional helicity increased linearly with μ_H (Figure 4). This means that a simple linear relation must also exist between helicity in water and helicity in bilayer. This provides a simple algorithm for estimating membrane-bound helicity from aqueous helicity (see Discussion).

The free energies of peptide partitioning into LUV formed from POPC and POPC/POPG (1:1) were determined both by CD and fluorescence spectroscopy titration following the procedures of White *et al.*[39] Typical titration data obtained by CD and fluorescence titration are included in Supplementary Material (Figs. S3 and S4). The data for all measurements are included in Supplementary Material (Table S2). Interestingly, the partitioning of the peptides into neutral and negatively charged lipids are very similar. For $A_8Q_3L_4$-5.54 for example, ΔG_{CD} = –7.0(±0.2) kcal mol^{-1} for the POPC LUV and –7.1(±0.2) kcal mol^{-1} for POPC/POPG as determined by CD spectroscopy. Similar values were obtained by fluorescence titration: ΔG_{CD} = –7.4(±0.2) kcal mol^{-1} for the POPC LUV and –7.2(±0.1) kcal mol^{-1} for POPC/POPG (Table S2). Overall, the results suggest that bilayer charge is irrelevant for the partitioning of these neutral peptides. The same is true for helicity. For example, fractional helicities f_α were computed from the values of $[\Theta]_{max}$ (see Methods), and found to be 73% and 75% for POPC and POPC/POPG, respectively (Figure 4) for $A_8Q_3L_4$-5.54.

Values of ΔG_{CD} for the peptides (see Supplementary Material, Table S2) are plotted against μ_H in Figure 6, which shows that the magnitudes of the partitioning free energies increase (become more favorable) linearly with μ_H. These results confirm that, within experimental errors, the partitioning of our neutral peptides is independent of

surface charge. A least-squares fit of the data to a linear curve thus yields a simple relationship between partitioning free energy and hydrophobic moment:

$$\Delta G_{CD} = -4.62(\pm 0.15) - 0.46(\pm 0.03)\mu_H \quad (1)$$

We examined the general validity of this equation by comparing the data of Figure 6 with partitioning free energy data for two peptides whose sequences and lengths differ dramatically from our 'Baldwin' peptides. The two peptides were the natural peptide melittin (26 residues: GIGAVLKVLTTGLPALISWIKRKRQQ-amide; μ_H = 5.18) and the designed peptide[31] TMX-3 (31 residues: GWAALAAHAAPALAAALAHAAASRSRSR-amide; μ_H = 3.32 at pH 7.6 and 4.25 at pH 6). The partitioning free energies of melittin[35] and TMX-3[31] are indicated in Figure 6 (open and closed circles, respectively. The agreement of these data with the $A_8Q_3L_4$-family data seems unimpressive until one considers the expected free energies based solely on total hydrophobicity (ΔG_{AB}): –0.07 kcal mol^{-1} for melittin; +0.75 kcal mol^{-1} for TMX-3 at pH 7.6; and +2.83 kcal mol^{-1} for TMX-3 at pH 6. Were it not for the amphiphilicity of these helical peptides, partitioning would be undetectable based upon simple hydrophobicity alone.

Interfacial Partitioning of Unfolded Peptides: ΔG_{AB}

The unfolded-peptide partitioning free energy ΔG_{AB} is the same for all of the peptides, because they all have the same amino acid composition. As described earlier, ΔG_{AB} is taken as equal to the partitioning free energy ΔG_{WW} calculated from the Wimley-White hydrophobicity scale[17] using the algorithm of Hristova and White[32] (**Table 1**). The computed value of ΔG_{AB} is –3.53 kcal mol^{-1}, which is considerably higher than the values of melittin and TMX-3.

Peptide folding in the membrane interface: ΔG_{BD}

The free energies of folding of the peptides in the interface were obtained by simple summation of the other legs of the thermodynamic cycle (summarized in Supplementary Material, Table S3). As shown in Figure 7a, ΔG_{BD} improves linearly with increases in μ_H, ranging from –0.25(±0.45) kcal mol^{-1} for $A_8Q_3L_4$–0.55 to –3.5(±0.07) kcal mol^{-1} for $A_8Q_3L_4$–5.54. Included in the figure are the estimated values of ΔG_{BD} for melittin and TMX-3 (pH 7.6). Not surprisingly, the values fall far off the curve for the $A_8Q_3L_4$ data. A possible explanation for the deviations is that melittin and TMX-3 have much longer sequences (n = 26 residues and 31 residues, respectively) than the $A_8Q_3L_4$

peptides (n = 17 residues, including the Gly-Trp residues at the C-terminal). This possibility gains credibility when the data are re-plotted using per-residue values of free energy, $\Delta G_{residue} = \Delta G_{BD}/f_{\alpha}n$, where f_{α} is the fractional helicity for fully bound peptides (above).

Values of $\Delta G_{residue}$ for melittin, TMX-3, and the $A_8Q_3L_4$ family are plotted against μ_H in Figure 7b. The $A_8Q_3L_4$ data are described well by the linear curve described by

$$\Delta G_{residue} = -0.10(\pm 0.03) - 0.029(\pm 0.007)\mu_H \quad (2)$$

$\Delta G_{residue}$ depends significantly upon μ_H, achieving a value of about –0.24 kcal mol^{-1} per residue for μ_H = 5. $\Delta G_{residue}$ folding free energies for TMX-3 and melittin are described remarkably well by the curve computed from the $A_8Q_3L_4$ data (**Eq. 2**).

DISCUSSION

We have examined the folding in water and membranes of a family of uncharged peptides of fixed amino acid composition (Ac-$A_8Q_3L_4$-GW-NH_2), designed to have different amphiphilicities as measured by the hydrophobic moment[1] (μ_H). We have shown that all of the peptides form α-helical secondary structure in both water and membranes. Because all of the peptides have the same hydrophobicity, differences in folding and binding free energies must be due to structural differences described by μ_H. In broad sweep, both helicity and membrane partitioning increased with μ_H, generally in a linear fashion (Figures 4 and 6). We used both neutral (POPC) and charged (POPC:POPG 1:1) LUV to see if partitioning and folding were affected by surface charge. They were not significantly affected (Figure 6).

As far as we are aware, this is the first examination of the helicity of peptides in buffer as a function of hydrophobic moment. Earlier studies of the contributions of non-polar residues to helix stability bear directly on the question of why the helicities of our peptides apparently depend upon hydrophobic moment. Without the aid of sidechain-sidechain helix-stabilizing interactions, only polyalanine readily forms stable helices in water[40]. Leucine-leucine (LL) pairs are among the non-polar side chain interactions that can contribute to the helical stability of soluble peptides[41], and (i, i + 4) LL pairs comprise the most frequently observed class of pair-wise side chain interactions in protein helices[42]. Formation of the interacting LL pair is assumed to be driven by non-polar contacts[43], probably by burial of non-polar surface area[44].

Recent results from Luo and Baldwin[45] have demonstrated that the (i, i + 4) LL interaction is substantially stronger than the (i, i + 3), probably because of differences in the solvation of peptide groups in the helix backbone. In their work, they used six different peptides: two as control and four with different side-chain interactions. Their data show that helicity increases with μ_H (see Supplementary Material, Table S4 and Figure S5). Two of our peptides, $A_8Q_3L_4$-5.51 and $A_8Q_3L_4$-5.54, have (i, i +3) and (i, i + 4) interactions, which may explain in part the dependence of helicity on μ_H.

Our data were collected systematically following the thermodynamic cycle of Figure 2a that uses the fully unfolded peptide state as the reference state. An important goal was to deduce the per-residue folding free energies of the $A_8Q_3L_4$ peptides in the membrane interface, ΔG_{BD}, by determining the energetics of the other three equilibria (ΔG_{AB}, ΔG_{AC}, and ΔG_{CD}). Because of the near-impossibility of measuring ΔG_{AB} directly[32], it was computed using the Wimley-White hydrophobicity scale[17] and the algorithm of Hristova and White[32]. ΔG_{AC} was measured by alcohol titration of peptides in buffer (Supplementary Material, Fig. S1) and found to decrease linearly as μ_H increased (Figure 5). ΔG_{CD} was determined for each peptide by CD spectroscopy and fluorescence titration methods (Figure 7 and Table 2. See also Supplementary Material, Figs. S3 and S4 and Table S2).

Our results lead to the conclusion that the amphiphilicity of helical peptides is dominant in the binding free energy in neutral membrane interfaces. This is apparent from the data shown in Figure 6. The partitioning free energies ΔG_{AB}, which measure only the hydrophobic affinity of unfolded peptides, vary from somewhat favorable for the $A_8Q_3L_4$ family (–3.53 kcal mol^{-1}) to barely favorable for melittin (–0.07 kcal mol^{-1}) to unfavorable for TMX-3 (+0.75 and +2.83 kcal mol^{-1}, pH 7.6 and pH 6.0, respectively). The amphiphilicities of the peptides apparently cause all of the peptides, regardless of sequence, to partition very strongly into the membrane interface. This means that the partitioning free energies of helical peptides cannot be predicted accurately based solely upon hydrophobicity. Accurate predictions require that hydrophobic moments be taken into account. Although the linear curve of Figure 6 does not describe the TMX-3 and melittin with great accuracy, it is clear that the best estimates of ΔG_{CD} for peptides will be obtained from hydrophobic moments rather than simple hydrophobicity considerations.

The process of designing new antimicrobial peptides is hindered by the time-consuming efforts required to synthesize, purify, and characterize candidate peptides.

An important subsidiary goal of our measurements was therefore to develop methods for designing peptides that will bind to membranes to a desired extent. The data presented here provide two practical approaches that apply to uncharged peptides partitioning into charged or uncharged membranes, or charged peptides partitioning into uncharged membranes. The inclusion of Coulombic interactions (below) adds an additional layer of complexity, but can be managed, in principle, by accounting for the non-additivity of hydrophobic and electrostatic interactions[28]. This is a subject for future work. The only purpose of the shortcuts outlined below is to minimize the number of rounds of design and experiment. Experimental verification of "predicted" physical parameters remains an essential step.

Designing Amphipathic Helices Using Hydrophobic Moments

As shown in Figure 6, the partitioning free energies decreased (became more favorable) linearly with μ_H, independent of the surface charge of the lipid. This seems to be a general result, because two peptides completely unrelated to the $A_8Q_3L_4$ (melittin and TMX-3) peptides are described reasonably well by the linear $\Delta G_{CD}(\mu_H)$ curve. However, because both melittin and TMX-3 are charged peptides, the relationship is applicable only to pure POPC bilayers, which is arguably the most widely used zwitterionic lipid. Although further refinements are in order, it appears that, to a reasonable approximation, ΔG_{CD} can be estimated from Eq. (1) given the hydrophobic moment.

Designing Amphipathic Helices Using Peptide Helicity

The linear dependence of helicity on μ_H (Figure 4) suggests that measured values of helicity can be useful for estimating the free energies of partitioning of peptides into uncharged LUV membranes using the thermodynamic cycle of Figure 2b. This is illustrated in Figure 8 where we have plotted ΔG_{CD} against the change in helicity Δf_α that accompanies partitioning of our peptides into POPC LUV. The linear dependence of ΔG_{CD} (kcal mol^{-1}) on Δf_α is described mathematically by

$$\Delta G_{CD} = -2.5(\pm 0.4) - 0.14(\pm 0.01)\, \Delta f_\alpha, \qquad (3)$$

where $\Delta f_\alpha = f_{m\alpha} - f_{w\alpha}$ and the subscripts m and w indicate membrane and water helicity values, respectively.

But without any measurements at all, it is possible to estimate helicity in water using the AGADIR algorithm of Muñoz and Serrano[46-49], which is based upon helix–coil transition theory and experimental measurements on 1200 peptides. The correlation between our measured values of aqueous helicity and values computed using AGADIR is quite good (see Supplementary Material, Fig. S6). Because of the implicit linear relationship between $f_{m\alpha}$ and $f_{w\alpha}$ shown in Figure 4, one can further estimate $f_{m\alpha}$ from the value of $f_{w\alpha}$ computed using AGADIR. Figure 9 shows the experimentally determined values of $f_{m\alpha}$ plotted against $f_{w\alpha}$ determined experimentally (■) or computed by AGADIR (○). A linear least-squares fit yields a linear relation between $f_{m\alpha}$ from the value of $f_{w\alpha}$ given by

$$f_{m\alpha} = 11.8(\pm 3.8) + 1.69(\pm 0.14) f_{w\alpha} \qquad (4)$$

Free Energy of Folding in Membrane Interfaces

In addition to establishing a practical general approach to peptide design, another goal of our experiments was to explore quantitatively the energetics of peptide folding in membrane interfaces. The free energy of folding of an unfolded peptide in the POPC bilayer interface, ΔG_{BD}, followed immediately from the sums of the other legs of the thermodynamic cycle of Figure 2a. ΔG_{BD} decreased linearly with increasing hydrophobic moment (Figure 7a). The resulting linear function, Eq. (2), does not appear to be generally useful, because ΔG_{BD} for melittin and for TMX3 fall well off of the curve in Figure 7a. This is not surprising, because melittin has 26 residues and TMX3 31 residues, while the Ac-$A_8Q_3L_4$-GW-NH_2 family has only 17. However, when peptide length is accounted for by calculating the per-residue free energy of folding using the equation $\Delta G_{residue} = \Delta G_{BD}/f_\alpha n$, both melittin and TMX-3 are described reasonably well by the $\Delta G_{residue}$ curve for the Ac-$A_8Q_3L_4$-GW-NH_2 family (Figure 7b). This suggests that Eq. (2) may be a general result useful for any peptide partitioning into neutral POPC interfaces. Unfortunately, there are very few partitioning free energy data available in the literature for testing this possibility. Future efforts to design peptides using the equations presented here should resolve the question.

Although the primary driving force for partitioning-folding coupling arises from the free energy reduction associated with peptide-bond hydrogen bonding, the dependence of $\Delta G_{residue}$ on μ_H indicates that other interactions must be important as well. These include as a minimum the effects of assembly entropy, sidechain packing,

relative exposure of sidechains to membrane and water, and the depth of membrane penetration by secondary structure units. This is apparent from the Li *et al.* study of the binding of fusion peptides to vesicle membranes[26].

The values of $\Delta G_{residue}$ for melittin found from direct measurements (**Fig. 7b**) or from Eq. (2) are –0.27(±0.01) and –0.29(±0.01) kcal mol^{-1} per residue, respectively, which are smaller than the value of –0.41(±0.06) kcal mol^{-1} determined by Ladokhin and White[23] from measurements of the partitioning of melittin and a diastereomeric melittin analog. There are two likely reasons for the difference: first, the diastereomer was not completely unfolded in the interface ($f_\alpha \approx 0.23$); second, Ladokhin and White assumed that $\Delta G_{AC} \approx 0$, which is contrary to our finding here that $\Delta G_{AC} \approx 1.6$ kcal mol^{-1} (see Supplementary Material, Table S1). This emphasizes the importance of using the thermodynamic cycle shown in Figure 2a. Interestingly, the revised value for melittin compares quite favorably with the value of –0.25(±0.05) kcal mol^{-1} per residue determined by Li *et al.*[26] for the partitioning of charged model host-guest fusion peptides partitioning into SUV formed from POPC:POPG (4:1). Because of the differences in experimental conditions, particularly charged peptides binding to charged SUV, the agreement is likely fortuitous. Similarly, the relatively small value of $\Delta G_{residue}$ of –0.14 kcal mol^{-1} per residue determined by Wieprecht and Seelig[25] for diastereomeric magainins is not easily compared directly with our results, because the binding free energies of the magainins to POPC:POPG also had a significant Coulombic component. In addition, they assumed hydrophobic and Coulombic free energies to be additive, which we now know to be an incorrect assumption[28]. Both the Li *et al.* and the Wieprecht and Seelig results involved extracting intrinsic (non-electrostatic) partition coefficients from the dependence of partitioning on surface potentials computed using the Gouy-Chapman equation[50]. This points out the need for extending studies of the μ_H-dependence of the partitioning of charged peptides into charged membranes.

MATERIALS AND METHODS

Materials

POPC and POPG were purchased from Avanti Polar Lipids (Alabaster, AL). Fmoc amino acids and resins for peptide synthesis were obtained from NovaBiochem (EMD Biosciences, San Diego, CA). All chemicals were of analytical reagent grade. A 10 mM potassium phosphate buffer solution (pH 7.0) was used to reduce the UV absorbance in CD experiments.

Peptide syntheses and purification

Peptides were synthesized on a 433A Applied Biosystems automatic synthesizer by step-wise solid-phase procedures[51] using fluorenylmethoxycarbonyl (F-moc) chemistry and TFA cleavage. Syntheses were performed on a 0.1 mmol scale starting with Fmoc-Rink amide MBHA resin. F-moc-protected amino acids were used for all coupling reactions. The crude peptides were purified by reverse-phase HPLC on a preparative C18 reverse-phase column using gradients of acetonitrile in 0.1% trifluoroacetic acid. Peptide identities were confirmed by matrix-assisted laser desorption ionization (MALDI) mass spectrometry (Chemistry Department, University of California, Irvine).

Peptide aggregation

Aqueous peptide concentrations of the peptides were typically 10-30 μM. We established by fluorescence and CD spectroscopy that the peptides were monomeric under the conditions of our experiments (data not shown). Specifically, CD spectra for all peptides were independent of concentration between ~15 and ~100 μM. Over the same concentration range, the wavelength of maximum fluorescence for Trp was found to be constant and equal to about 350 nm, as expected for aqueous solutions of monomeric peptides.

Preparation of vesicles

A defined amount of lipid in chloroform was first dried under nitrogen and then overnight under high vacuum. Typically, 1-2 mL of buffer was added to the lipid and the dispersion vortexed extensively. Large unilamellar vesicles (LUV, diameter ~ 0.1 μm) were formed under nitrogen by extrusion through Nucleopore polycarbonate membranes (ten times through two stacked 0.1-μm filters), using the method of Mayer *et al.*[52]

Circular Dichroism and Optical Absorbance

CD measurements were performed using an upgraded Jasco-720 spectropolarimeter (Japan Spectroscopic Company, Tokyo). Normally, 10 to 30 scans were recorded between 190 and 260 nm at ambient temperature (~25°C), using a 1 mm optical path. All spectra were corrected for background scattering by subtracting a vesicle-only spectrum measured with an appropriate concentration of vesicles in

buffer, without the peptide. Measured values of ellipticity (Θ) were converted into the ellipticity per amino acid residue [Θ] using

$$[\Theta] = \frac{\Theta MW_R}{lc}, \tag{5}$$

where l is the optical path-length of the cell, c the peptide concentration, and MW_R the average mass per amino acid residue of the peptide used.

The fractional helical content f_α was estimated using the formula

$$f_\alpha = \frac{\Theta - \Theta_{RC}}{\Theta_H - \Theta_{RC}}, \tag{6}$$

where Θ is the observed ellipticity, Θ_{RC} the limiting value for a completely random coil, and Θ_H the limiting value for a completely helical conformation. We determined from titrations of our peptides with 2,2,2-trifluoroethanol (TFE) that $[\Theta]_{222}$ for 100% and 0% helicity have been estimated as –33,050 deg cm^2 dmol^{-1} and –1,500 deg cm^2 dmol^{-1}, respectively (see Supplementary Material, Fig. S2). The value determined for Θ_H is satisfyingly close to the theoretically expected value of -33,529 computed from data and analysis of Chen et al.[53]. CD spectra and absorbance were measured in the same cuvette in order to minimize errors in determination of molar ellipticity. UV absorbance was measured with a Cary 3E spectrophotometer (Varian Analytical Instruments, Sugar Land, TX). Molar concentrations were determined using a molar extinction coefficient of ε_{280nm} = 5600 M^{-1} cm^{-1} for tryptophan. Peptide concentrations were typically between 10 and 30 μM in phosphate buffer.

Fluorescence measurements

Fluorescence was measured using an OLIS-modified SLM-Aminco 8100 steady-state fluorescence spectrometer (Jobin Yvon, Edison, NJ, formerly SLM/Aminco, Urbana, IL) equipped with double-grating excitation and single-grating emission monochromators. All measurements were made in 2 × 10 mm cuvettes in a room thermostated to 25°C. Cross-orientation of polarizers was used (excitation polarization set to horizontal, emission polarization set to vertical) to minimize the scattering contributions from

vesicles and to eliminate spectral polarization effects in monochromator transmittance. Peptide concentrations ranged from 10 to 15 μM.

Data analysis

Hydrophobic moments (μ_H) were determined using the Totalizer module of Membrane Protein Explorer (MPEx) available online at http://blanco.biomol.uci.edu/mpex. Totalizer computes μ_H using the formula[54]

$$\mu_H = \left\{ \left[\sum_{n=1}^{N} H_n \sin(\delta n) \right]^2 + \left[\sum_{n=1}^{N} H_n \cos(\delta n) \right]^2 \right\}^{\frac{1}{2}}, \quad (7)$$

where N is the number of residues in the sequence segment, H_n is the numerical value of hydrophobicity of the nth amino acid residue from the Wimley-White interfacial hydrophobicity scale[17], $\delta = 2\pi/m$, and m is the number of residues per turn. We assume an α-helix with $m = 3.6$ residues per turn, which yields $\delta = 100°$.

Free energies of transfer ΔG of the peptides were determined from mole-fraction partition coefficients K_x using $\Delta G = -RT\ln K_x$, where K_x is given by

$$K_x = \frac{([P]_{bil}/[L])}{([P]_{water}/[W])} \quad (8)$$

in which $[P]_{bil}$ and $[P]_{water}$ are the bulk molar concentrations of peptide attributable to peptide in the bilayer and water phases, respectively. $[L]$ and $[W]$ are the molar concentrations of lipid and water (55.3M). Given that $[P]_{total} = [P]_{bil} + [P]_{water}$, one can easily show that

$$f_p = \frac{K_x[L]}{[W] + K_x[L]}, \quad (9)$$

where f_p is the fraction of peptide bound. K_x was determined by least-squares fitting of eq. 8 to plots of f_p against $[L]$ using the Origin 7.0 software package (OriginLab, Inc., Northampton, MA).

The fraction of peptide bound was determined by titration measurements using both CD and fluorescence measurements. These methods have been described in detail by White *et al.*[39] For CD measurements we used

$$\Theta_{norm} = 1 + \left(\Theta_m - 1\right)\frac{K_x[L]}{[W] + K_x[L]}, \tag{10}$$

where Θ_{norm} is the normalized molar ellipticity of the peptide and Θ_m is the maximum normalized molar ellipticity of the peptide in the membrane.

For fluorescence titrations, K_x was determined from fluorescence intensities (I) that were fitted[35,39] by standard non-linear least-squares methods to

$$I = 1 + \left(I_\infty - 1\right)\frac{K_x[L]}{[W] + K_x[L]}, \tag{11}$$

where I is the normalized fluorescence intensity of the peptide at the chosen wavelength and I_∞ is the maximum normalized intensity of the peptide in the membrane.

ACKNOWLEDGEMENTS

We thank Michael Myers for his editorial assistance and Drs. Hirsh Nanda and Ryan Benz for providing coordinates from the simulation of melittin in a bilayer. Research supported by the National Institute of General Medical Sciences, US National Institutes of Health.

Supplementary Data

Supplementary data associated with this article can be found in the online version.

REFERENCES

1. Eisenberg, D., Weiss, R. M. & Terwilliger, T. C. (1982). The helical hydrophobic moment: A measure of the amphiphilicity of a helix. *Nature* **299**, 371-374.

2. Rees, D. C., De Antonio, L. & Eisenberg, D. (1989). Hydrophobic organization of membrane proteins. *Science* **245**, 510-513.

3. Granseth, E., von Heijne, G. & Elofsson, A. (2005). A study of the membrane-water interface region of membrane proteins. *J. Mol. Biol.* **346**, 377-385.

4. Kuo, A., Gulbis, J. M., Antcliff, J. F., Rahman, T., Lowe, E. D., Zimmer, J., Cuthbertson, J., Ashcroft, F. M., Ezaki, T. & Doyle, D. A. (2003). Crystal structure of the potassium channel KirBac1.1 in the closed state. *Science* **300**, 1922-1926.

5. Long, S. B., Campbell, E. B. & MacKinnon, R. (2005). Voltage sensor of Kv1.2: Structural basis of electromechanical coupling. *Science* **309**, 903-908.

6. Inaba, K., Murakami, S., Suzuki, M., Nakagawa, A., Yamashita, E., Okada, K. & Ito, K. (2006). Crystal structure of the DsbB-DsbA complex reveals a mechanism of disulfide bond generation. *Cell* **127**, 789-801.

7. Zhong, L., Putnam, R. J., Johnson, W. C., Jr. & Rao, A. G. (1995). Design and synthesis of amphipathic antimicrobial peptides. *Int. J. Pept. Protein Res.* **45**, 337-347.

8. Dathe, M., Wieprecht, T., Nikolenko, H., Handel, L., Maloy, W. L., MacDonald, D. L., Beyermann, M. & Bienert, M. (1997). Hydrophobicity, hydrophobic moment and angle subtended by charged residues modulate antibacterial and haemolytic activity of amphipathic helical peptides. *FEBS Lett.* **403**, 208-212.

9. Tossi, A., Tarantino, C. & Romeo, D. (1997). Design of synthetic antimicrobial peptides based on sequence analogy and amphipathicity. *Eur. J. Biochem.* **250**, 549-558.

10. Wieprecht, T., Dathe, M., Krause, E., Beyermann, M., Maloy, W. L., MacDonald, D. L. & Bienert, M. (1997). Modulation of membrane activity of amphipathic, antibacterial peptides by slight modifications of the hydrophobic moment. *FEBS Lett.* **417**, 135-140.

11. Dathe, M. & Wieprecht, T. (1999). Structural features of helical antimicrobial peptides: Their potential to modulate activity on model membranes and biological cells. *Biochim. Biophys. Acta* **1462**, 71-87.

12. Tossi, A., Sandri, L. & Giangaspero, A. (2000). Amphipathic, α-helical antimicrobial peptides. *Biopolymers (Pept. Sci.)* **55**, 4-30.

13. Kaiser, E. T. & Kézdy, F. J. (1983). Secondary structures of proteins and peptides in amphiphilic environments (A review). *Proc. Natl. Acad. Sci. USA* **80**, 1137-1143.

14. Kaiser, E. T. & Kézdy, F. J. (1984). Amphiphilic secondary structure: Design of peptide hormones. *Science* **223**, 249-255.

15. Sargent, D. F., Bean, J. W. & Schwyzer, R. (1988). Conformation and orientation of regulatory peptides on lipid membranes Key to the molecular mechanish of receptor selection. *Biophys. Chem.* **31**, 183-193.

16. Maloy, W. L. & Kari, U. P. (1995). Structure-activity studies on magainins and other host defense peptides. *Biopolymers* **37**, 105-122.

17. Wimley, W. C. & White, S. H. (1996). Experimentally determined hydrophobicity scale for proteins at membrane interfaces. *Nat. Struct. Biol.* **3**, 842-848.

18. Wimley, W. C., Hristova, K., Ladokhin, A. S., Silvestro, L., Axelsen, P. H. & White, S. H. (1998). Folding of β-sheet membrane proteins: A hydrophobic hexapeptide model. *J. Mol. Biol.* **277**, 1091-1110.

19. Habermann, E. (1972). Bee and wasp venoms. *Science* **177**, 314-322.

20. Vogel, H. (1981). Incorporation of melittin into phosphatidylcholine bilayers: Study of binding and conformational changes. *FEBS Lett.* **134**, 37-42.

21. Kuchinka, E. & Seelig, J. (1989). Interaction of melittin with phosphatidylcholine membranes. Binding isotherm and lipid head-group conformation. *Biochemistry* **28**, 4216-4221.

22. Beschiaschvili, G. & Baeuerle, H.-D. (1991). Effective charge of melittin upon interaction with POPC vesicles. *Biochim. Biophys. Acta* **1068**, 195-200.

23. Ladokhin, A. S. & White, S. H. (1999). Folding of amphipathic α-helices on membranes: Energetics of helix formation by melittin. *J. Mol. Biol.* **285**, 1363-1369.

24. Oren, Z. & Shai, Y. (1997). Selective lysis of bacteria but not mammalian cells by diastereomers of melittin: Structure-function study. *Biochemistry* **36**, 1826-1835.

25. Wieprecht, T., Apostolov, O., Beyermann, M. & Seelig, J. (1999). Thermodynamics of the α-helix-coil transition of amphipathic peptides in a membrane environment: Implications for the peptide-membrane binding equilibrium. *J. Mol. Biol.* **294**, 785-794.

26. Li, Y., Han, X. & Tamm, L. K. (2003). Thermodynamics of fusion peptide-membrane interactions. *Biochemistry* **42**, 7245-7251.

27. Dathe, M., Schümann, M., Wieprecht, T., Winkler, A., Beyermann, M., Krause, E., Matsuzaki, K., Murase, O. & Bienert, M. (1996). Peptide helicity and membrane surface charge modulate the balance of electrostatic and hydrophobic interactions with lipid bilayers and biological membranes. *Biochemistry* **35**, 12612-12622.

28. Ladokhin, A. S. & White, S. H. (2001). Protein chemistry at membrane interfaces: Non-additivity of electrostatic and hydrophobic interactions. *J. Mol. Biol.* **309**, 543-552.

29. Chakrabartty, A. & Baldwin, R. L. (1995). Stability of α-helices. *Adv. Protein Chem.* **46**, 141-176.

30. White, S. H. & Wimley, W. C. (1999). Membrane protein folding and stability: Physical principles. *Annu. Rev. Biophys. Biomol. Struc.* **28**, 319-365.

31. Ladokhin, A. S. & White, S. H. (2004). Interfacial folding and membrane insertion of a designed helical peptide. *Biochemistry* **43**, 5782-5791.

32. Hristova, K. & White, S. H. (2005). An experiment-based algorithm for predicting the partitioning of unfolded peptides into phosphatidylcholine bilayer interfaces. *Biochemistry* **44**, 12614-12619.

33. Hirota, N., Mizuno, K. & Goto, Y. (1997). Cooperative α-helix formation of β-lactoglobulin and melittin induced by hexafluoroisopropanol. *Protein Sci.* **6**, 416-421.

34. Hirota, N., Mizuno, K. & Goto, Y. (1998). Group additive contributions to the alcohol-induced α-helix formation of melittin: Implication for the mechanism of the alcohol effects on proteins. *J. Mol. Biol.* **275**, 365-378.

35. Ladokhin, A. S., Jayasinghe, S. & White, S. H. (2000). How to measure and analyze tryptophan fluorescence in membranes properly, and why bother? *Anal. Biochem.* **285**, 235-245.

36. Serrano, L. (2000). The relationship between sequence and structure in elementary folding units. *Adv. Protein Chem.* **53**, 49-85.

37. Chakrabartty, A., Kortemme, T., Padmanabhan, S. & Baldwin, R. L. (1993). Aromatic side-chain contribution to the far-ultraviolet circular dichroism of helical peptides and its effect on measurement of helix propensities. *Biochemistry* **32**, 5560-5565.

38. Hessa, T., Kim, H., Bihlmaier, K., Lundin, C., Boekel, J., Andersson, H., Nilsson, I. M., White, S. H. & von Heijne, G. (2005). Recognition of transmembrane helices by the endoplasmic reticulum translocon. *Nature* **433**, 377-381.

39. White, S. H., Wimley, W. C., Ladokhin, A. S. & Hristova, K. (1998). Protein folding in membranes: Determining the energetics of peptide-bilayer interactions. *Meth. Enzymol.* **295**, 62-87.

40. Rohl, C. A., Chakrabartty, A. & Baldwin, R. L. (1996). Helix propagation and N-cap propensities of the amino acids measured in alanine-based peptides in 40 volume percent trifluoroethanol. *Protein Sci.* **5**, 2623-2637.

41. Padmanabhan, S. & Baldwin, R. L. (1994). Tests for helix-stabilizing interactions between various nonpolar side chains in alanine-based peptides. *Protein Sci.* **3**, 1992-1997.

42. Klingler, T. M. & Brutlag, D. L. (1994). Discovering structural correlations in α-helices. *Protein Sci.* **3**, 1847-1857.

43. Creamer, T. P. & Rose, G. D. (1995). Interactions between hydrophobic side chains within α-helices. *Protein Sci.* **4**, 1305-1314.

44. Avbelj, F. & Fele, L. (1998). Role of main-chain electrostatics, hydrophobic effect and side-chain conformational entropy in determining the secondary structure of proteins. *J. Mol. Biol.* **279**, 665-684.

45. Luo, P. & Baldwin, R. L. (2002). Origin of the different strengths of the (i,i+4) and (i,i+3) leucine pair interactions in helices. *Biophys. Chem.* **96**, 103-108.

46. Muñoz, V. & Serrano, L. (1995). Elucidating the folding problem of helical peptides using empirical parameters. II. Helix macrodipole effects and rational modification of the helical content of natural peptides. *J. Mol. Biol.* **245**, 275-296.

47. Muñoz, V. & Serrano, L. (1995). Elucidating the folding problem of helical peptides using empirical parameters. III. Temperature and pH dependence. *J. Mol. Biol.* **245**, 297-308.

48. Muñoz, V. & Serrano, L. (1997). Development of the multiple sequence approximation within the AGADIR model of α-helix formation: Comparison with Zimm-Bragg and Lifson-Roig formalisms. *Biopolymers* **41**, 495-509.

49. Lacroix, E., Viguera, A. R. & Serrano, L. (1998). Elucidating the folding problem of α-helices: Local motifs, long-range electrostatics, ionic-strength dependence and prediction of NMR parameters. *J. Mol. Biol.* **284**, 173-191.

50. McLaughlin, S. (1989). The electrostatic properties of membranes. *Ann. Rev. Biophys. Biophys. Chem.* **18**, 113-136.

51. Stewart, J. M. & Young, J. D. (1984). *Solid Phase Peptide Synthesis*, Pierce, Rockford, IL.

52. Mayer, L. D., Hope, M. J. & Cullis, P. R. (1986). Vesicles of variable sizes produced by a rapid extrusion procedure. *Biochim. Biophys. Acta* **858**, 161-168.

53. Chen, Y.-H., Yang, J. T. & Chau, K. H. (1974). Determination of the helix and β form of proteins in aqueous solution by circular dichroism. *Biochemistry* **13**, 3350-3359.

54. Eisenberg, D., Weiss, R. M. & Terwilliger, T. C. (1984). The hydrophobic moment detects periodicity in protein hydrophobicity. *Proc. Natl. Acad. Sci. USA* **81**, 140-144.

55. Benz, R. W., Nanda, H., Castro-Román, F., White, S. H. & Tobias, D. J. (2006). Diffraction-based density restraints for membrane and membrane/protein molecular dynamics simulations. *Biophys. J.* **91**, 3617-3629.

56. Humphrey, W., Dalke, W. & Schulten, K. (1996). VMD: Visual molecular dynamics. *J. Mol. Graph.* **14**, 33-38.

FIGURE LEGENDS

Figure 1. Amphipathic helices at membrane interfaces. Residues are colored according to residue type: yellow, non-polar; green, polar; blue, basic; red, acidic. The non-polar residues generally face the hydrocarbon interior of the bilayer while the polar and charged residues face the aqueous phase. (**a**) Melittin, an archetypal toxin peptide, embedded in the interface of a dioleoylphosphatidylcholine (DOPC) bilayer. The image was created from a frame taken from a restrained molecular dynamics simulation[55]. (**b**) Channel domain of the KirBac1.1 ligand-gated K^+-channel in the closed state[4], including the interfacial slide helices that mechanically couple the ligand receptor (not shown) to channel opening. Amphipathic helices such as these are common structural features of membrane proteins[2,3]. Images produced with VMD software[56].

Figure 2. Thermodynamic schemes for peptide partitioning and folding in membrane interfaces. (**a**) Four-state thermodynamic cycle for describing the partitioning and folding of peptides into bilayer interfaces from water using four states: fully unfolded peptide in the aqueous phase (state A) and in the membrane (state B), partially folded in aqueous phase (state C), and folded in the membrane interface (state D). This scheme takes the fully unfolded peptide in the aqueous phase as the reference state. As we state before, measurements of the partitioning of most biologically interesting peptides yield free energies for the C to D equilibrium, because the B state is much less populated than the D state. Nevertheless, the A to B equilibrium establishes an important reference state. (**b**) Two-state thermodynamic cycle commonly used for describing peptide partitioning into the membrane interface. Three thermodynamic states are shown: partially folded in water (state C), partially folded in membrane (state C'), and folded in the membrane interface (state D). The C' state cannot generally be observed experimentally by the usual optical methods because its occupancy is very small compared to state D. This thermodynamic scheme is a very practical one, because the C and D states (and therefore ΔG_{CD}) are readily accessible by circular dichroism and fluorescence measurements. But the difficulty is that each peptide has a different degree of folding in the aqueous and membrane phases, which

complicates the per-residue folding free energy in the interface. The scheme in **panel a** avoids this problem by tying all measures to a common reference state.

Figure 3. CD spectra of the peptides $A_8Q_3L_4$-5.51, $A_8Q_3L_4$-2.86, and $A_8Q_3L_4$-0.55 at 25 °C in 10 mM phosphate buffer, and 20-30 μM peptide. The spectra were taken in a 1-mm path length cuvette and averaged over 10-20 scans. Increasing the hydrophobic moment increases the helical content in water (measured as molar ellipticity at 222 nm).

Figure 4. Helicity of the $A_8Q_3L_4$-family of peptides in water and the membrane interface (POPC solid down-side triangles and POPC:POPG open down-side triangles) as a function of hydrophobic moment. Helicity is a linear function of hydrophobic moment in both media, and it does not depend on the lipid surface charge. Helicity in the membrane interface was determined from $[\Theta_{max}]$ computed from binding curves. See Methods and Supplementary Figure S3.

Figure 5. The linear dependence of the free energy of helix formation in water as a function of hydrophobic moment.

Figure 6. The free energy of partitioning (ΔG_{CD}) the $A_8Q_3L_4$-family of peptides into POPC (solid red circles) and POPC:POPG (solid black squares) LUV interfaces. The solid line is the best-fit linear curve through all points. Partitioning free energy values for TMX-3 (31-residues: GWAALAAHAAPALAAALAHAAASRSRSR-amide; μ_H = 3.32 at pH 7.6 and 4.25 at pH 6) and melittin (26 residues: GIGAVLKVLTTGLPALISWIKRKRQQ-amide; μ_H = 5.18) are included for comparison (closed and open circles, respectively). The TMX-3 and melittin free energies are not described particularly well by the linear curve, which is not surprising given the great differences in sequence and length compared to the $A_8Q_3L_4$-family. More important, however, is the fact that both TMX-3 and melittin have little tendency to partition into POPC interfaces based upon total hydrophobicity (see text).

Figure 7. Free energies of folding of the $A_8Q_3L_4$-family of peptides in the POPC interface. (**a**) Values of free energy ΔG_{BD} of folding in the POPC interface computed using the thermodynamic scheme of Figure 2a and the computed values for ΔG_{AB}

(Table 1, $\Delta G_{AB} \equiv \Delta G_{WW}$) and the measured values of ΔG_{AC} and ΔG_{CD}. The corresponding values of melittin and TMX-3 (solid circle and solid square, respectively) fall far off the curve. This appears in large measure to be due to sequence length. (**b**) The data of **panel a** re-plotted using per-residue free energies $\Delta G_{residue}$ computed from $\Delta G_{residue} = \Delta G_{BD}/f_{\alpha}n$, where f_{α} is the fractional helicity and n is the number of residues in the sequence. Notice that the TMX-3 and melittin data are described reasonably well by the $A_8Q_3L_4$ when length is accounted for, computed as follows: Melittin has a 6% helix content in aqueous solution that increases to $f_{\alpha} = 0.71$ when membrane-bound[20,23]. We determined experimentally that $\Delta G_{AC} = 1.62(\pm 0.06)$ kcal mol^{-1} (data not shown), and computed from the Hristova-White algorithm[32] computed that $\Delta G_{AB} = -0.07$ kcal mol^{-1}. From these values, the value of ΔG_{CD} (see text), and $n = 26$, $\Delta G_{residue}$ is found to be $-0.27(\pm 0.01)$ kcal mol^{-1} per residue. TMX-3 has a 22% helix content in aqueous solution, which increases to about 70% when membrane–bound at neutral pH. We determined experimentally (data not shown) that $\Delta G_{AC} = 0.74(\pm 0.03)$ kcal mol^{-1}. From these values, the value of ΔG_{CD} (see text), and $n = 31$, we computed $\Delta G_{residue}$ as $-0.24(\pm 0.01)$ kcal mol^{-1} for TMX-3 in the deprotonated form. This value is approximate, because ΔG_{AC} was determined only at neutral pH where the amino terminus and the His residues are still partially protonated.

Figure 8. The free energy of partitioning of the $A_8Q_3L_4$ family of peptides from buffer to the POPC bilayer interface plotted as a function of the difference in helicity (Δf_{α}) of the peptides in the membrane and in water (Figure 4).

Figure 9. The helicity of the $A_8Q_3L_4$ family of peptides in membranes $f_{m\alpha}$ plotted against the fractional helicities $f_{w\alpha}$ in buffer. The experimentally determined values of $f_{m\alpha}$ plotted against $f_{w\alpha}$ determined experimentally (■) or computed by AGADIR (○).

Table 1. Amino acid sequences of the $A_8Q_3L_4$ family of peptides used in this study, including computed hydrophobic moments and partitioning free energies.

Amino Acid Sequence	Name	[a]Hydrophobic moment (μ_H)	[b]ΔG_{WW} (kcal mol^{-1})
Ac-LQALAAQALQAAALA-GW-NH_2	$A_8Q_3L_4$-0.55	0.55	–3.53
Ac-LAQAAALQLLAAQAA-GW-NH_2	$A_8Q_3L_4$-2.00	2.00	–3.53
Ac-AQLAALAALQAAQLA-GW-NH_2	$A_8Q_3L_4$-2.86	2.86	–3.53
Ac-AAAQAAAQLLQALLA-GW-NH_2	$A_8Q_3L_4$-4.72	4.72	–3.53
Ac-QLAQALAAALAALAQ-GW-NH_2	$A_8Q_3L_4$-5.51	5.51	–3.53
Ac-QALQALAAALAALAQ-GW-NH_2	$A_8Q_3L_4$-5.54	5.54	–3.53

[a]Hydrophobic moments were computed using the Totalizer module of MPEx, available over the World Wide Web: http://blanco.biomol.uci.edu/mpex

[b]Free energies of transfer from water to bilayer interface based upon the Wimley-White[17] experiment-based interfacial hydrophobicity scale. These were also computed using the Totalizer module of MPEx (above).

Figure 1

Click here to download high resolution image

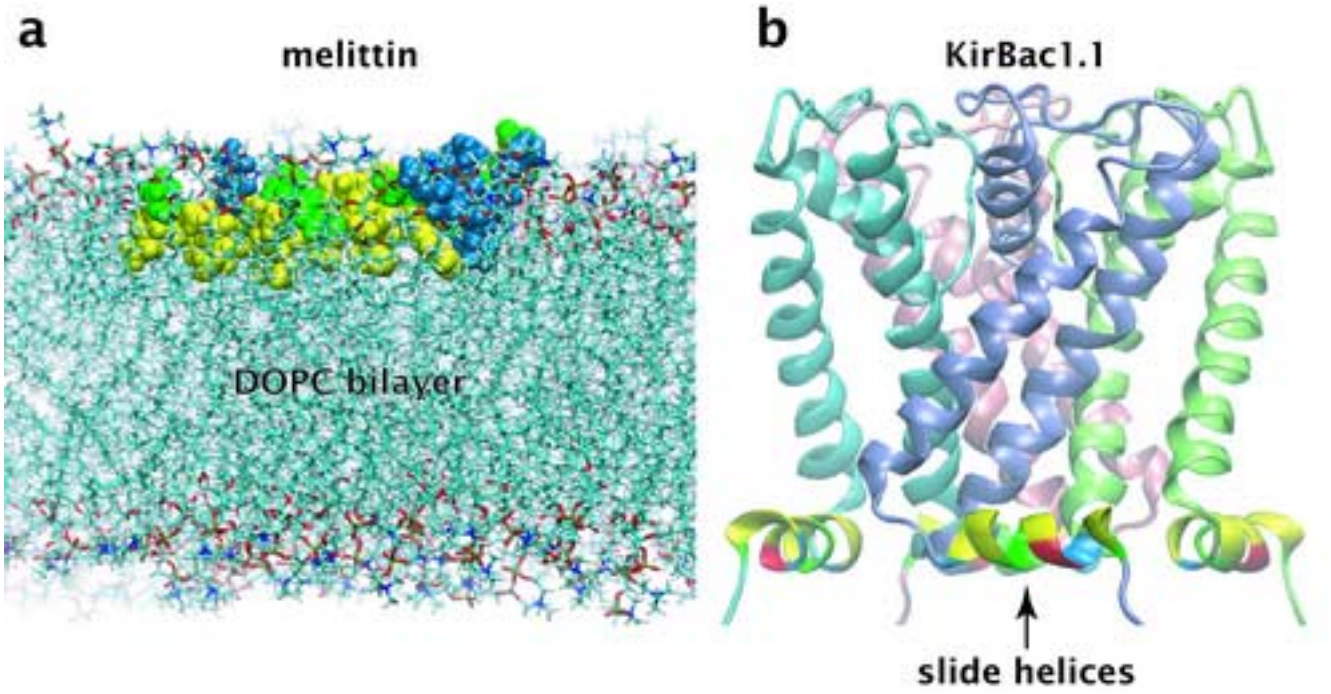

Figure 2

Click here to download high resolution image

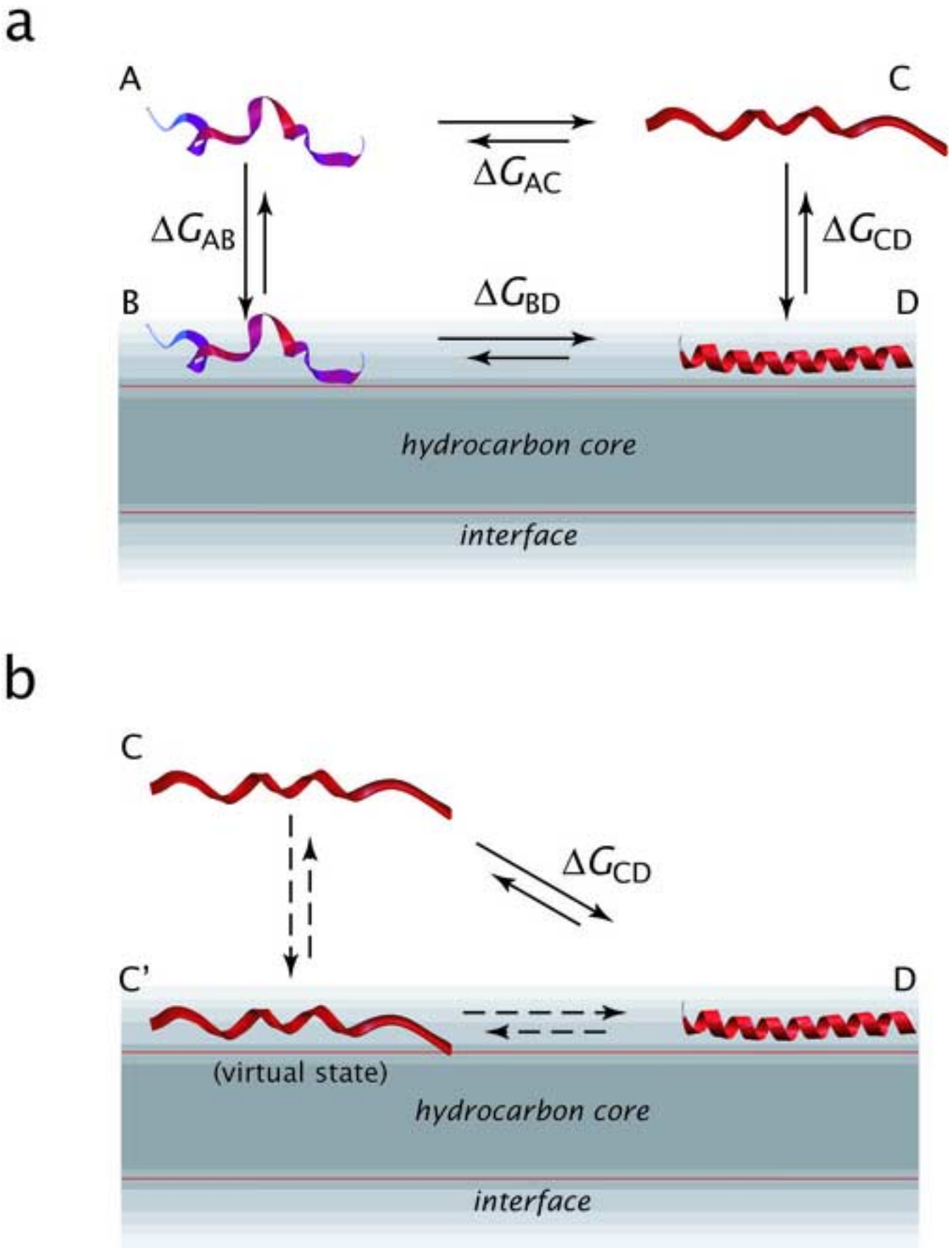

Figure 3

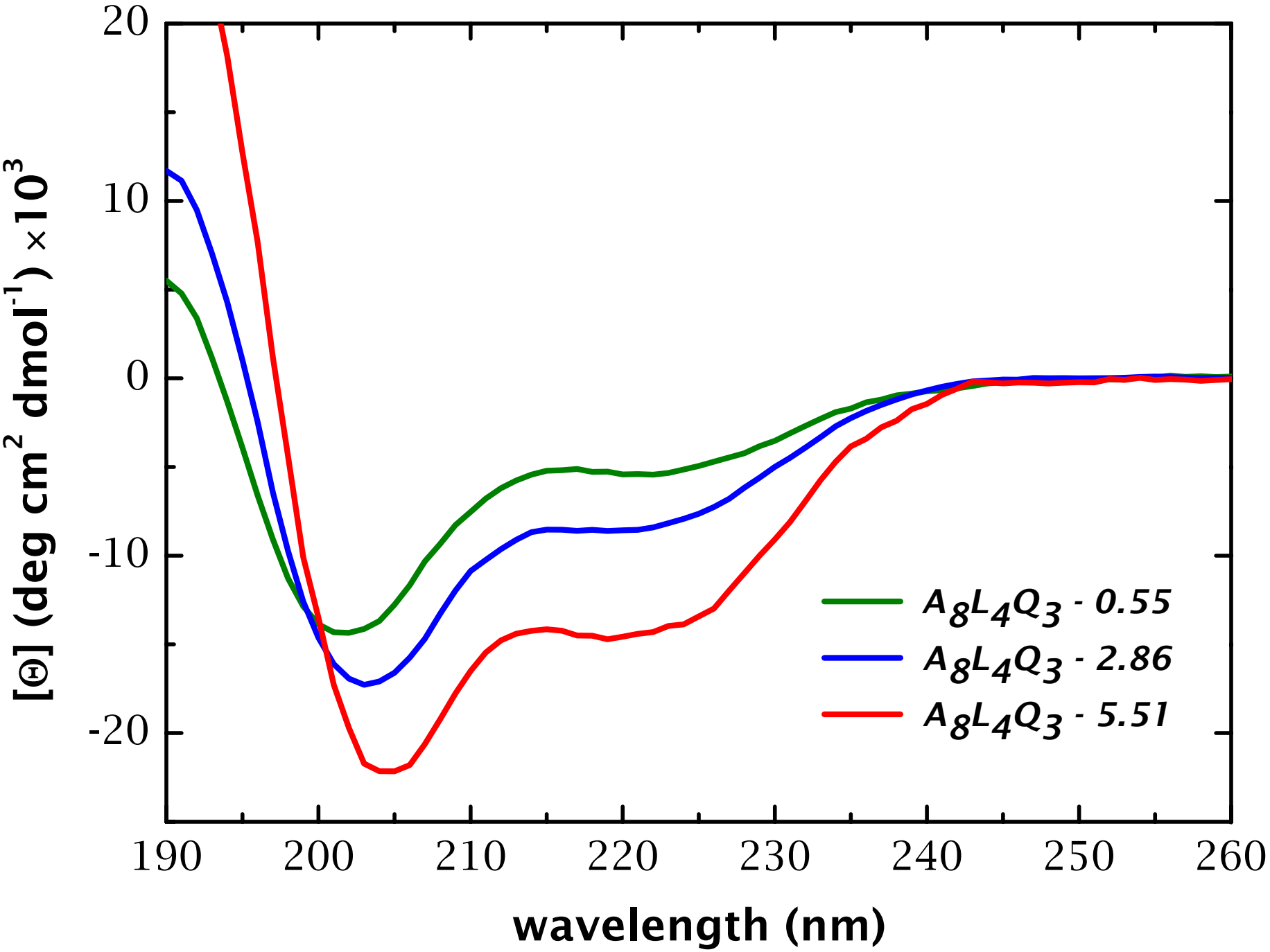
20
10
0
-10
-20
190
200
210
220
230
240
250
260
[Θ] (deg cm^2 dmol^{-1}) ×10^3
wavelength (nm)
$A_8L_4Q_3$ - 0.55
$A_8L_4Q_3$ - 2.86
$A_8L_4Q_3$ - 5.51

Figure 4

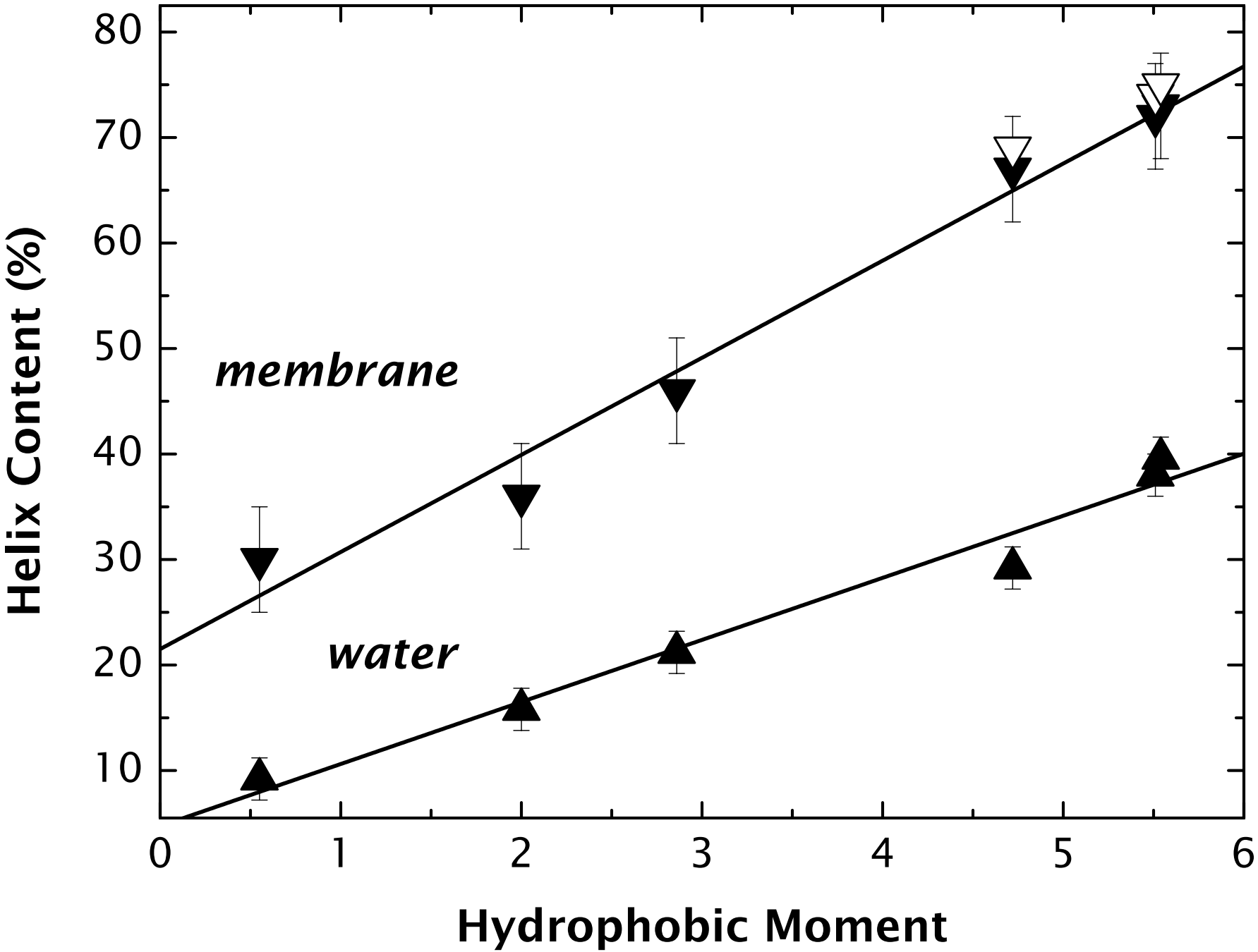
Helix Content (%)
80
70
60
50
40
30
20
10
membrane
water
0
1
2
3
4
5
6
Hydrophobic Moment

Figure 5

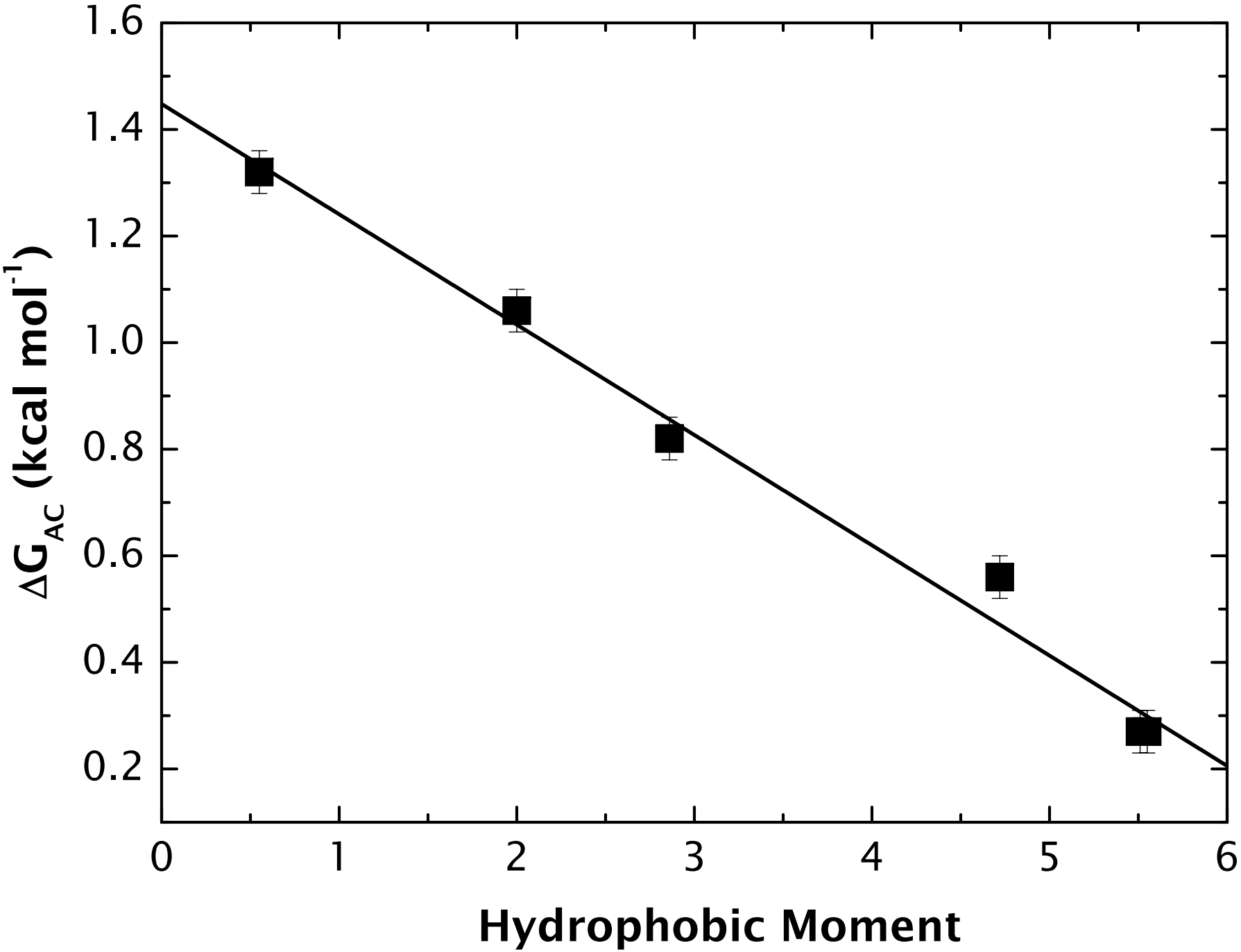
1.6
1.4
1.2
1.0
0.8
0.6
0.4
0.2
ΔG_AC (kcal mol^-1)
0
1
2
3
4
5
6
Hydrophobic Moment

Figure 6

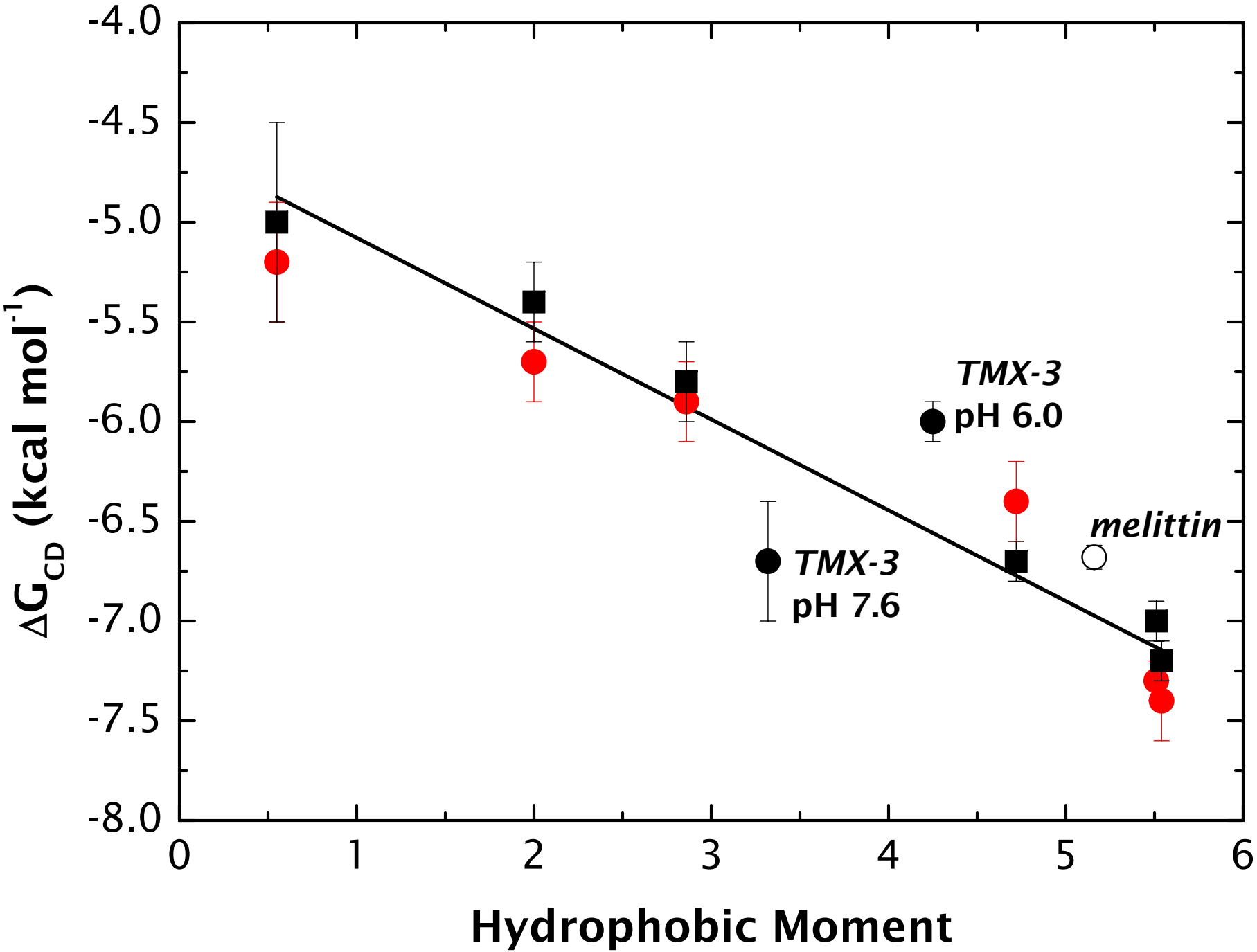
-4.0
-4.5
-5.0
-5.5
-6.0
-6.5
-7.0
-7.5
-8.0
0
1
2
3
4
5
6
ΔG_CD (kcal mol^-1)
Hydrophobic Moment
TMX-3
pH 6.0
TMX-3
pH 7.6
melittin

Figure 7

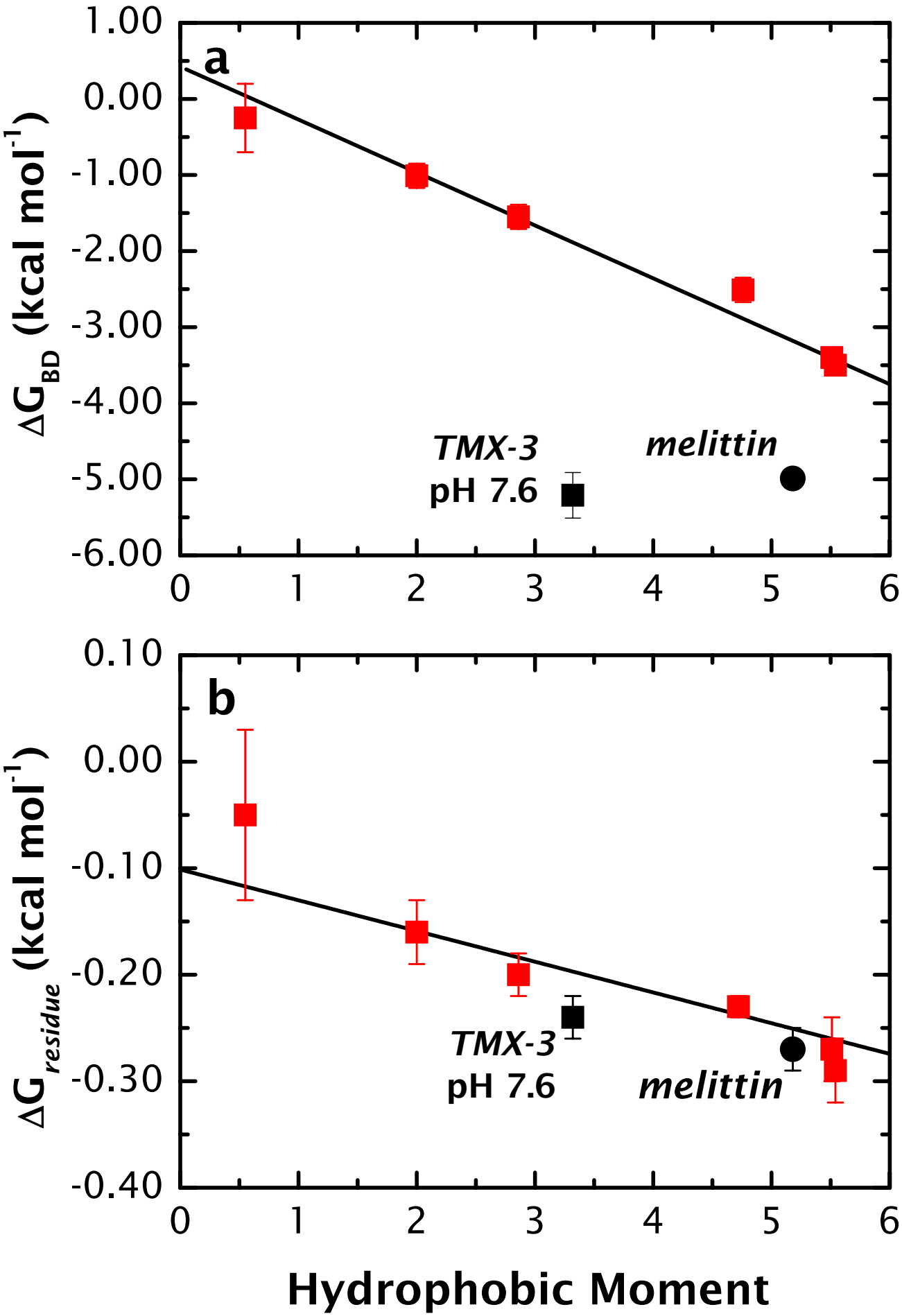
a
b
1.00
0.00
-1.00
-2.00
-3.00
-4.00
-5.00
-6.00
0.10
0.00
-0.10
-0.20
-0.30
-0.40
0
1
2
3
4
5
6
ΔG_BD (kcal mol^-1)
ΔG_residue (kcal mol^-1)
TMX-3
pH 7.6
melittin
Hydrophobic Moment

Figure 8

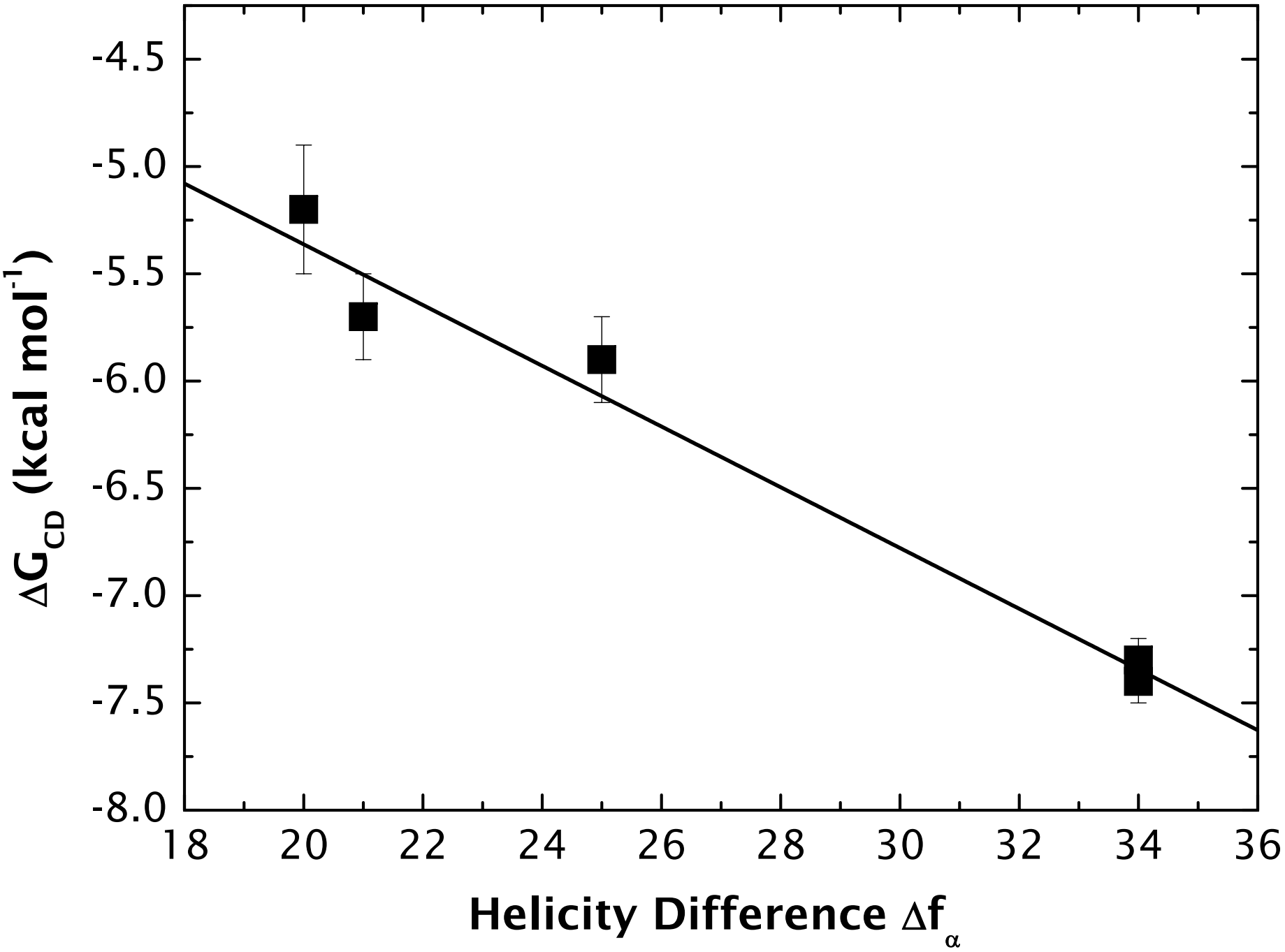
-4.5
-5.0
-5.5
-6.0
-6.5
-7.0
-7.5
-8.0
18
20
22
24
26
28
30
32
34
36
ΔG_CD (kcal mol^-1)
Helicity Difference Δf_α

Figure 9

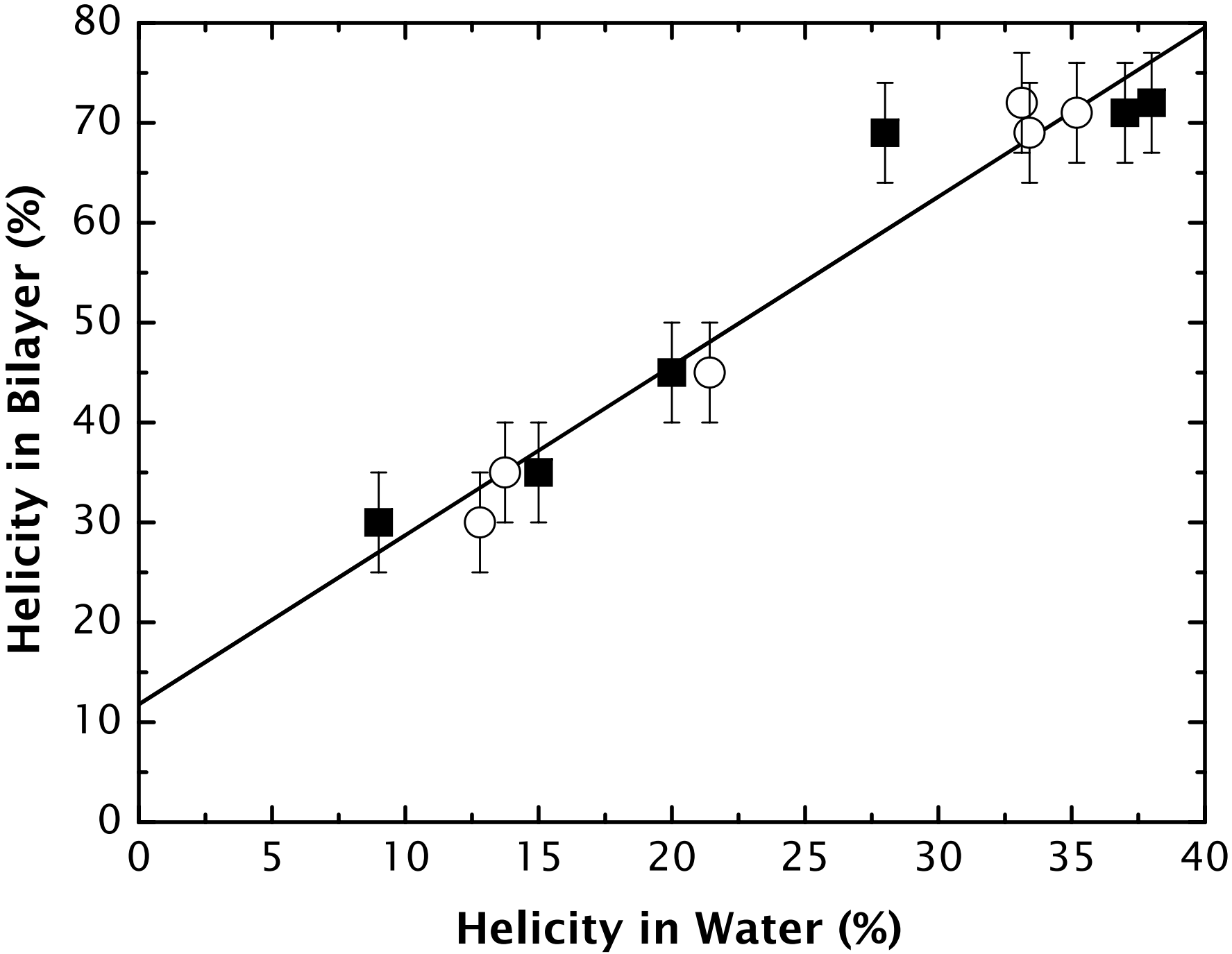
Helicity in Bilayer (%)
Helicity in Water (%)
0
10
20
30
40
50
60
70
80
0
5
10
15
20
25
30
35
40

Journal of Molecular Biology, JMB-D-07-00422

Online Supplementary Data

FOLDING AMPHIPATHIC HELICES INTO MEMBRANES: AMPHIPHILICITY TRUMPS HYDROPHOBICITY

Mónica Fernández-Vidal[1,4], Sajith Jayasinghe[2], Alexey S. Ladokhin[3], and Stephen H. White[1]

[1]Department of Physiology and Biophysics, University of California at Irvine, Irvine, CA 92697-4560, USA. [2]Department of Chemistry and Biochemistry, California State University at San Marcos, San Marcos, CA 92096, USA. [3]Department of Biochemistry and Molecular Biology, University of Kansas Medical Center, Kansas City, KS 66160-7421, USA. [4]Present address: Dept. of Peptide and Protein Chemistry, IIQAB-CSIC, 08034 Barcelona, Spain. Correspondence should be addressed to S.H.W. (stephen.white@uci.edu) or A.S.L. (aladokhin@kumc.edu).

Folding of the $A_8Q_3L_4$ family of peptides in buffer

In order to calculate the free energies of folding of the $A_8Q_3L_4$ family of peptides in water, we used the alcohol-induced α-helix formation method of Hirota *et al.*[1,2] We approximated the alcohol-induced transition by a two-state mechanism, *i.e.*, the only states present are the native and the α-helical states for all the peptides. The CD spectra of the titrations of peptides with 2,2,2-trifluoroethanol (TFE) showed an isodichroic point at ~ 203 nm (**Fig. S1**), consistent with a two-state approximation.

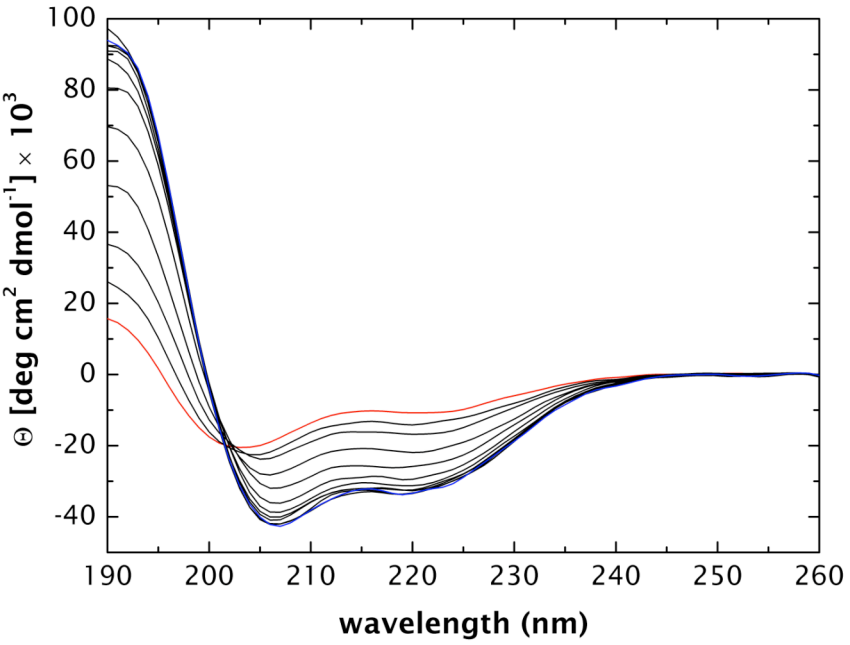

Figure S1. CD spectra of $A_8Q_3L_4$-4.72 in buffer with increasing additions of trifluoroethanol (TFE), ranging from 0.0 M (red curve) to 5.5 M (blue curve). Notice the isodichroic point at ~203 nm.

Analysis of two-state alcohol-induced folding of unfolded or partially folded peptides[3] follows the same methods used for analyzing the two-state denaturation of soluble proteins using a chaotropic agent, such as urea. A good description of the use of denaturation for studying the stability of soluble proteins is given by Goldenberg[4]. The parameter we follow for alcohol-induced folding is the molar ellipticity at 222 nm, $[\Theta]_{222}$. Plots of $[\Theta]_{222}$ against alcohol concentration follows a Boltzmann distribution, as shown below. A side benefit of this method is that one can estimate the ellipticities

for fully folded and fully unfolded peptides, Θ_H and Θ_{RC}, respectively, which are necessary for determining the fractional ellipticities f_α using eq. (6).

The free energy change ΔG_0 for folding in the absence of TFE is given by $\Delta G_0 = -RT\ln K_0 \equiv \Delta G_{AC}$, where $K_0 = f_\alpha(0)/f_u(0)$ (see **Table S1**, below). The terms $f_\alpha(0)$ and $f_u(0)$ indicate the fractions of folded and unfolded peptide, respectively, for [TFE] = 0.

For [TFE] ≠ 0, the free energy of folding ΔG_F can be described[2,3] by

$$\Delta G_F = \Delta G_0 - m[\mathrm{TFE}] \tag{S1}$$

where m measures the dependence of ΔG_F on TFE concentration. Rearrangement of eq. S1 after substitution of the definitions of ΔG_F and ΔG_0 yields

$$K_F = K_0 \exp(m[\mathrm{TFE}]/RT) \tag{S2}$$

It follows from $K_F = f_\alpha/(1-f_\alpha)$ that

$$f_\alpha = K_F/(1+K_F) = 1/(1+K_F^{-1}) \tag{S3}$$

Substitution of eq. S2 into eq. S3 yields

$$f_\alpha = 1/(1 + K_0^{-1} \exp(-m[\mathrm{TFE}]/RT)) \tag{S4}$$

Eq. S4 is the Boltzmann function. One can readily show that $f_\alpha = f_\alpha(0)$ for [TFE] = 0, $f_\alpha \rightarrow 1$ as [TFE] becomes large and positive, and $f_\alpha \rightarrow 0$ as [TFE] becomes large and negative. Of course, [TFE] cannot be less than 0, but for the purpose of curve fitting that does not matter. Because S4 is the Boltzmann function, one can fit molar ellipticity data $[\Theta]_{222}([\mathrm{TFE}])$ to a general Boltzmann fitting function using non-linear least squares methods. Defining [TFE] = c, Θ_H and Θ_{RC} can be determined from

$$[\Theta]_{222} = \frac{\Theta_{RC} - \Theta_H}{1 + \exp\left(c/\Delta c\right)} + \Theta_H \tag{S5}$$

where Δc is a parameter that describes the width of the transition from f_u to f_α as the TFE concentration is increased.

Each peptide of the family was titrated with TFE and methanol (data not shown) at T = 298 K, and the resulting data fitted to eq. S5. The results are shown in **Fig. S2**.

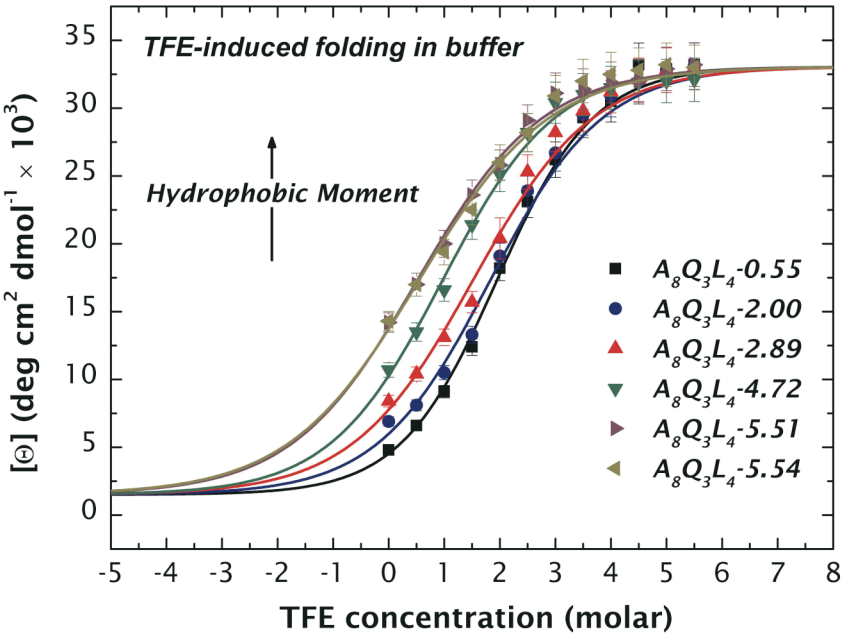

Figure S2. Plots of molar ellipticity versus TFE concentration for the $A_8Q_3L_4$ family of peptides. Notice that all peptides are maximally folded in ≈ 6 M TFE. From these data, we established that Θ_{RC} = -1500 and Θ_H = -33050 deg cm^2 dmol^{-1}. Because Θ_H is the same for all of the peptides, we assume that Θ_H corresponds to 100% helicity. This assumption is supported by the comprehensive data and analysis of Chen et al.[5]. Their Equation (2) used with parameters from their Table IV yield a theoretical value of Θ_H = -33529 deg cm^2 dmol^{-1}, which is satisfyingly close to our value.

From these data, we obtained values of ΔG_{AC} and $f_\alpha(0)$, which are summarized in **Table S1**.

Table S1. Helicities and folding free energies (ΔG_{AC}) in buffer for the $A_8Q_3L_4$ family of peptides and for melittin. The free energy change ΔG_0 for folding in the absence of TFE is given by $\Delta G_0 = -RT\ln K_0 \equiv \Delta G_{AC}$, where $K_0 = f_\alpha(0)/f_u(0)$. The terms $f_\alpha(0)$ and $f_u(0)$ indicate the fractions of folded and unfolded peptide, respectively, for [TFE] = 0 M.

[a]Peptide	[b]Θ_{222}	[c]Measured f_α	[d]Computed f_α	ΔG_{AC} (kcal mol^{-1})	[e]$\Delta G_{per\ residue}$ (kcal mol^{-1})
$A_8Q_3L_4$-0.55	–4400	0.092	0.13	1.32±0.06	0.84±0.02
$A_8Q_3L_4$-2.00	–6500	0.158	0.14	1.06±0.04	0.39±0.01
$A_8Q_3L_4$-2.86	–8200	0.212	0.21	0.82±0.04	0.23±0.01
$A_8Q_3L_4$-4.72	–10700	0.292	0.33	0.56±0.04	0.11±0.01
$A_8Q_3L_4$-5.51	–13500	0.380	0.35	0.27±0.04	0.042±0.006
$A_8Q_3L_4$-5.54	–14000	0.396	0.33	0.27±0.04	0.040±0.006
melittin	–3000	0.060	0.013	1.62±0.06	1.04±0.04
TMX-3	-6500	0.220	0.031	0.74±0.03	0.11±0.01

[a]See Table 1

[b]molar ellipticity, deg cm^2 dmol^{-1}

[c]fractional helicity in buffer. See Methods.

[d]fractional helicity, determined using the computer program AGADIR[6-9]. The estimated uncertainty in these values is estimated by the authors of AGADIR to be 6%.

[e]These are per-residue free energies computed using $\Delta G_{per\ residue} = \Delta G_{AC}/f_\alpha n$, where f_α is the fractional helicity and n is the number of residues in the sequence.

Determination of the partitioning free energies into membranes of partially-folded peptides

The free energies of peptide partitioning into LUV formed from POPC and POPC/POPG (1:1) were determined by both CD and fluorescence spectroscopy titration following the procedures of White *et al.*[10] (see Methods). The results are summarized in **Table S2**, below.

Typical titration data obtained by CD spectroscopy in **Fig. S3** for $A_8L_4Q_3$–5.54, where the upper panels (**A and B**) correspond to a titration with POPC membranes and the lower panels (**C and D**) to titrations with POPC/POPG membranes. The helicity of $A_8L_4Q_3$–5.54 increases steadily with additions of lipid (**panels A and C**). Molar ellipticity at 222 nm was used to determine quantitatively partitioning isotherms[10-12]. These were fit by least-squares minimization to obtain the maximum ellipticity ($[\Theta]_{max}$), and mole-fraction partition coefficients (K_x) and consequently ΔG_{CD} (**panels B and D**), as described in Methods.

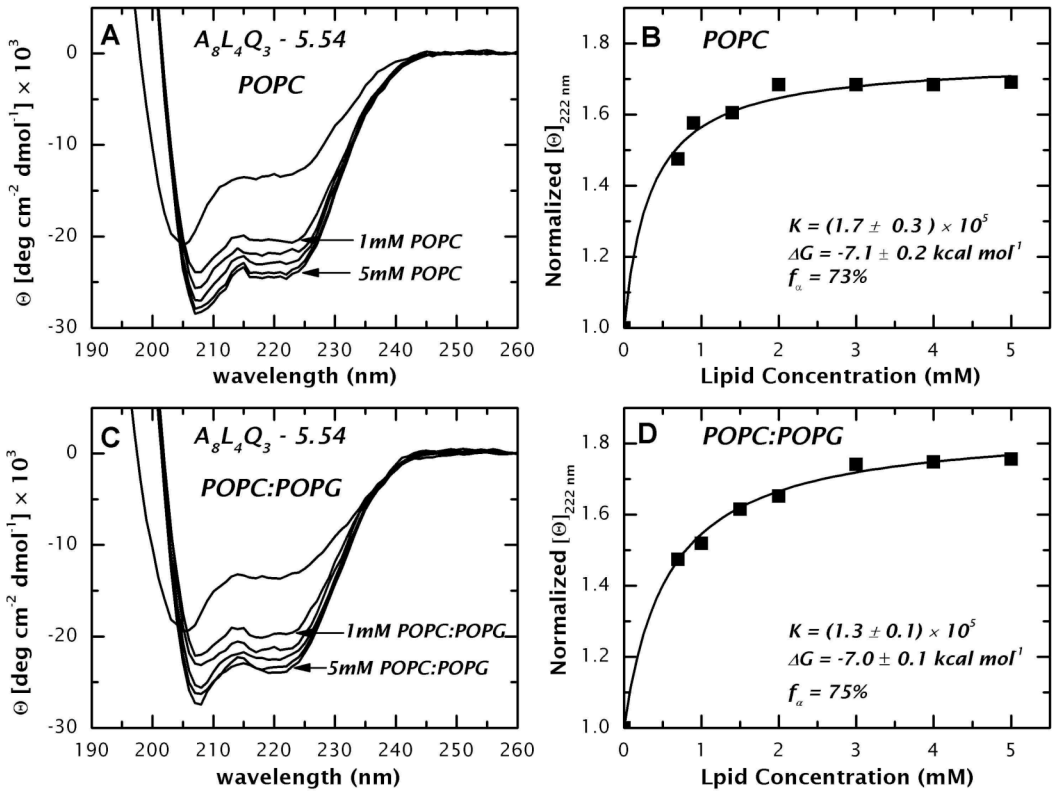

Figure S3. Typical titration data obtained by CD spectroscopy for $A_8L_4Q_3$–5.54, where the upper panels (**A and B**) correspond to a titration with POPC membranes and the lower panels (**C and D**) to titrations with POPC/POPG membranes

Because Trp fluorescence is sensitive to its dielectric environment, membrane association of peptides results in a blue-shift in the Trp fluorescence wavelength

maximum (λ_{max}) that can be used to measure membrane partitioning[10] by titration of peptide solutions with LUV, as discussed in detail by Ladokhin *et al.*[13]. Typical fluorescence spectra and titration data are presented for $A_8L_4Q_3$–5.54 in **Fig. S4**. All spectra were corrected for scattering artifacts[13]. For both POPC and POPC/POPG (**panels A and C**, respectively), λ_{max} = 350 nm in buffer, shifting to about 335 nm in the presence of lipid. Titration curves obtained from the change in fluorescence at 325 nm are shown in panels B and D for POPC and POPC/POPG, respectively. In a manner similar to that for the CD titrations, the data shown in **Fig. S4** were fit by least-squares minimization to obtain the mole-fraction partition coefficient K_X and the maximum intensity increase I_∞ (**panels B and D**), as described in Methods.

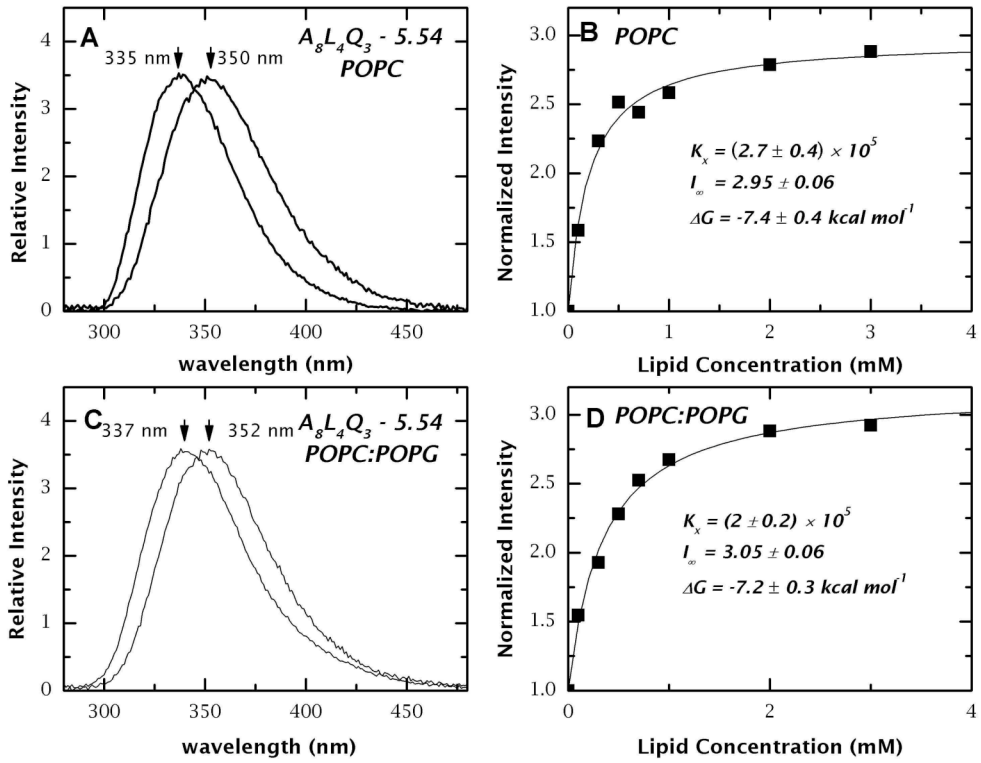

Figure S4. Typical fluorescence spectra and titration data for $A_8L_4Q_3$–5.54. All spectra were corrected for scattering artifacts[13]. For both POPC and POPC/POPG (**panels A and C**, respectively), λ_{max} = 350 nm in buffer, shifting to about 335 nm in the presence of lipid. Binding curves determined from data such as those of panels A and C (see Methods) are shown in **panels B and D** for POPC and POPC:POPG, respectively.

Table S2. Free energies of transfer ΔG_{CD} of the $A_8Q_3L_4$ family of peptides from buffer into neutral and anionic large unilamellar vesicles.

[a]Peptide	[b]Θ_{222}	[c]f_α	[d]ΔG_{CD} POPC	[d]ΔG_{CD} [e]POPC:POPG	[d]ΔG_{CD} POPC	[d]ΔG_{CD} [e]POPC:POPG
			[f]*Fluorescence Titration*		[f]*CD Titration*	
$A_8Q_3L_4$-0.55	–12000	0.30	–5.2±0.3	–5.0±0.5	—	—
$A_8Q_3L_4$-2.00	–13000	0.36	–5.7±0.2	–5.4±0.2	—	—
$A_8Q_3L_4$-2.86	–16000	0.46	–5.9±0.2	–5.8±0.2	—	—
$A_8Q_3L_4$-4.72	–22000	0.67	–6.4±0.2	–6.7±0.1	–6.1±0.1	–6.1±0.1
$A_8Q_3L_4$-5.51	–24500	0.72	–7.3±0.1	–7.0±0.1	–7.3±0.2	–7.1±0.2
$A_8Q_3L_4$-5.54	–25000	0.73	–7.4±0.2	–7.2±0.1	–7.0±0.2	–7.1±0.2

[a]see Table 1

[b]maximum molar ellipticity [Θ_{max}] deg $cm^2 dmol^{-1}$ (see Fig. S3).

[c]fractional helicity obtained by CD experiments (see Methods). When CD experiments were not possible, approximations were made from ellipticities of titrations of the peptides with methanol.

[d]kcal mol^{-1}

[e]POPC:POPG = 1:1

[f]see Methods

Peptide folding in the membrane interface: ΔG_{BD}

The free energies of folding of the peptides in the interface are obtained by simple summation of the other legs of the thermodynamic cycle shown in **Fig. 1a**. The results are summarize in **Table S3**, below.

Table S3. Free energy of folding ΔG_{BD} in the POPC bilayer interface.

[a]Peptide	[b]ΔG_{BD} kcal mol^{-1}	[c]$\Delta G_{residue}$ kcal mol^{-1}
$A_8Q_3L_4$-0.55	–0.35±0.30	–0.07±0.06
$A_8Q_3L_4$-2.00	–1.11±0.20	–0.18±0.03
$A_8Q_3L_4$-2.86	–1.55±0.20	–0.20±0.02
$A_8Q_3L_4$-4.72	–2.51±0.20	–0.23±0.02
$A_8Q_3L_4$-5.51	–3.50±0.11	–0.28±0.01
$A_8Q_3L_4$-5.54	–3.60±0.11	–0.29±0.02
Melittin-5.16	–5.31±0.21	–0.27±0.01
TMX3-3.32 pH=7.6	-7.21±0.20	-0.24±0.02

[a]Table 1

[b]Computed from the thermodynamic cycle of **Fig. 1a** and the data of **Tables 1**, **S1**, and **S2**.

[c]These are per-residue free energies computed using $\Delta G_{residue} = \Delta G_{AC}/f_{\alpha}n$, where f_{α} is the fractional helicity (**Table S2**) and n is the number of residues in the sequence.

Leu-Leu interactions and helix stability

Table S4. Sequences of peptides used by Luo and Baldwin[14] for studying the role of Leu-Leu interactions in helix stability. Even in this case, the helicity in water increases with the hydrophobic moment (**Fig. S5**).

Sequence	Sidechain interaction	[a]f_α	[b]μH
Ac-KAAAAKAALAKLAAAKGY-NH_2	(i,i+3)	26%	0.57
Ac-KAAAAKAALAKALAAKGY-NH_2	(i,i+4)	37%	1.33
Ac-ELAALKAKLAALKAKAGY-NH_2	2(i,i+3) + (i,i+4)	46%	1.48
Ac-ELAALKAKLAALKAKLGY-NH_2	2(i,i+3) + 2(i,i+4)	53%	1.62

[a] Percentage values given by Luo and Baldwin[14] of helical content in buffer.

[b] Values of hydrophobic moment computed by MPEx.

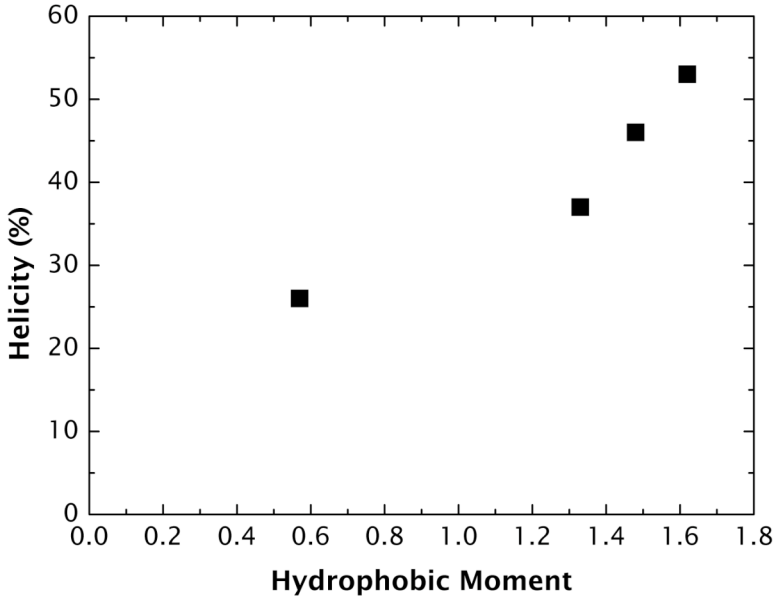

Figure S5. Plot the helicities in **Table S4** versus hydrophobic moment.

Consistency of the measured values of helix content with values calculated using AGADIR

As shown below in **Fig. S6**, the relation between the measured values of helicity and values computed with AGADIR[6-9] is described well by a straight line forced through the origin (y = ax). The slope of the curve is 1.03(±0.03). This means that AGADIR is useful for estimating helicities in water. For instance, the peptide $A_8L_4Q_3$-0.55 is 9% helical in water, while AGADIR predicts 12.8 % ± 6%.

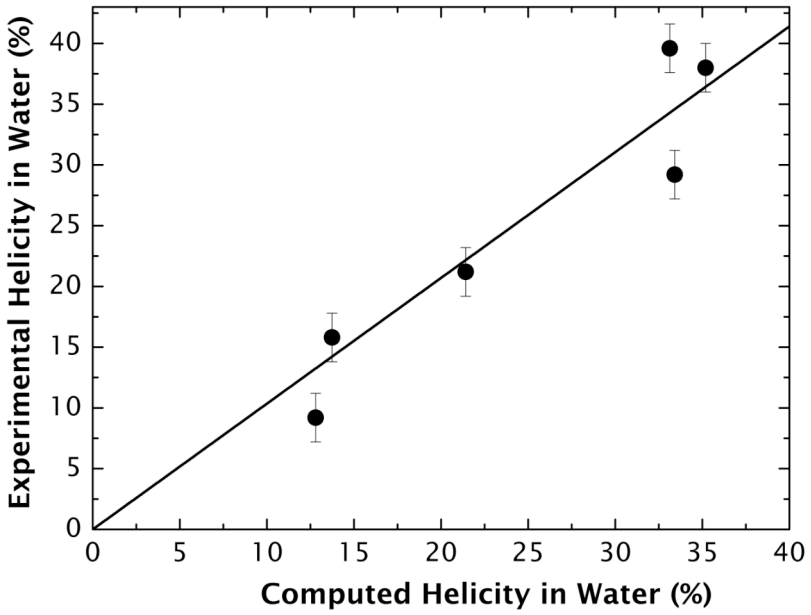

Figure S6. Experimentally determined helical content for the $A_8L_4Q_3$ peptide family in water plotted against helical contents computed using the program Agadir[6-9].

References

1. Hirota, N., Mizuno, K. & Goto, Y. (1997). Cooperative α-helix formation of β-lactoglobulin and melittin induced by hexafluoroisopropanol. *Protein Sci.* **6**, 416-421.

2. Hirota, N., Mizuno, K. & Goto, Y. (1998). Group additive contributions to the alcohol-induced α-helix formation of melittin: Implication for the mechanism of the alcohol effects on proteins. *J. Mol. Biol.* **275**, 365-378.

3. Jasanoff, A. & Fersht, A. R. (1994). Quantitative determination of helical propensities from trifluoroethanol titration curves. *Biochemisty* **33**, 2129-2135.

4. Goldenberg, D. P. (1992). Mutational analysis of protein folding and stability. In *Protein Folding* (Creighton, T. E., ed.), pp. 353-403. W. H. Freeman, New York.

5. Chen, Y.-H., Yang, J. T. & Chau, K. H. (1974). Determination of the helix and β form of proteins in aqueous solution by circular dichroism. *Biochemistry* **13**, 3350-3359.

6. Muñoz, V. & Serrano, L. (1995). Elucidating the folding problem of helical peptides using empirical parameters. II. Helix macrodipole effects and rational modification of the helical content of natural peptides. *J. Mol. Biol.* **245**, 275-296.

7. Muñoz, V. & Serrano, L. (1995). Elucidating the folding problem of helical peptides using empirical parameters. III. Temperature and pH dependence. *J. Mol. Biol.* **245**, 297-308.

8. Muñoz, V. & Serrano, L. (1997). Development of the multiple sequence approximation within the AGADIR model of α-helix formation: Comparison with Zimm-Bragg and Lifson-Roig formalisms. *Biopolymers* **41**, 495-509.

9. Lacroix, E., Viguera, A. R. & Serrano, L. (1998). Elucidating the folding problem of α-helices: Local motifs, long-range electrostatics, ionic-strength dependence and prediction of NMR parameters. *J. Mol. Biol.* **284**, 173-191.

10. White, S. H., Wimley, W. C., Ladokhin, A. S. & Hristova, K. (1998). Protein folding in membranes: Determining the energetics of peptide-bilayer interactions. *Meth. Enzymol.* **295**, 62-87.

11. Rizzo, V., Stankowski, S. & Schwarz, G. (1987). Alamethicin incorporation in lipid bilayers: A thermodynamic study. *Biochemistry* **26**, 2751-2759.

12. Schwarz, G. & Beschiaschvili, G. (1989). Thermodynamic and kinetic studies on the association of melittin with a phospholipid bilayer. *Biochim. Biophys. Acta* **979**, 82-90.

13. Ladokhin, A. S., Jayasinghe, S. & White, S. H. (2000). How to measure and analyze tryptophan fluorescence in membranes properly, and why bother? *Anal. Biochem.* **285**, 235-245.

14. Luo, P. & Baldwin, R. L. (2002). Origin of the different strengths of the (i,i+4) and (i,i+3) leucine pair interactions in helices. *Biophys. Chem.* **96**, 103-108.

Control CD and Fluorescence Data for the $A_8Q_3L_4$ family of peptides in buffer

Not for Publication

FOLDING AMPHIPATHIC HELICES INTO MEMBRANES: AMPHIPHILICITY TRUMPS HYDROPHOBICITY

Mónica Fernández-Vidal[1,4], Sajith Jayasinghe[2], Alexey S. Ladokhin[3], and

Stephen H. White[1]

[1]Department of Physiology and Biophysics, University of California at Irvine, Irvine, CA 92697-4560, USA. [2]Department of Chemistry and Biochemistry, California State University at San Marcos, San Marcos, CA 92096, USA. [3]Department of Biochemistry and Molecular Biology, University of Kansas Medical Center, Kansas City, KS 66160-7421, USA. [4]Present address: Dept. of Peptide and Protein Chemistry, IIQAB-CSIC, 08034 Barcelona, Spain. Correspondence should be addressed to S.H.W. (stephen.white@uci.edu) or A.S.L. (aladokhin@kumc.edu).

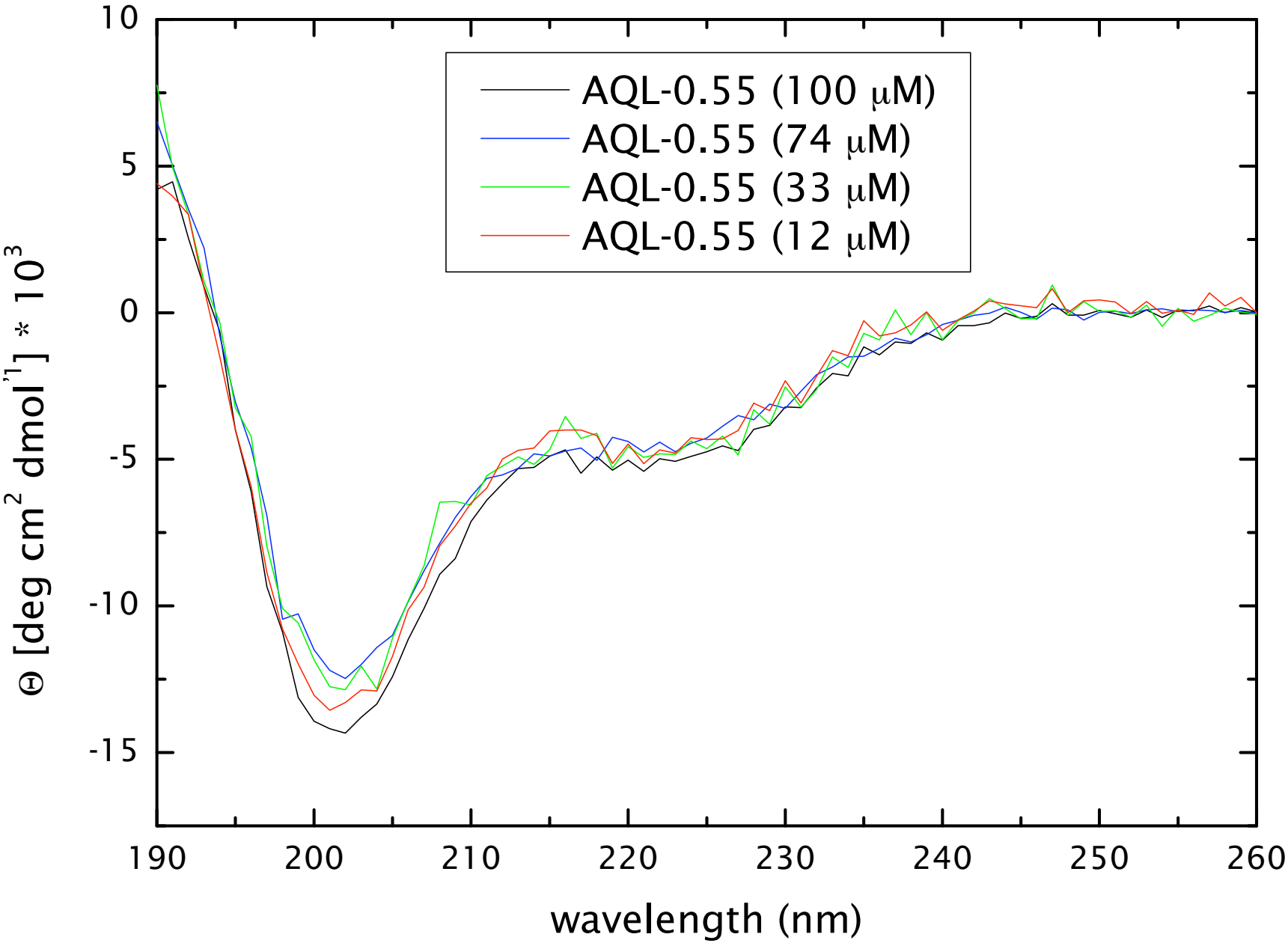
AQL-0.55 (100 μM)
AQL-0.55 (74 μM)
AQL-0.55 (33 μM)
AQL-0.55 (12 μM)
Θ [deg cm2 dmol'1] * 10^3
wavelength (nm)
10
5
0
-5
-10
-15
190
200
210
220
230
240
250
260

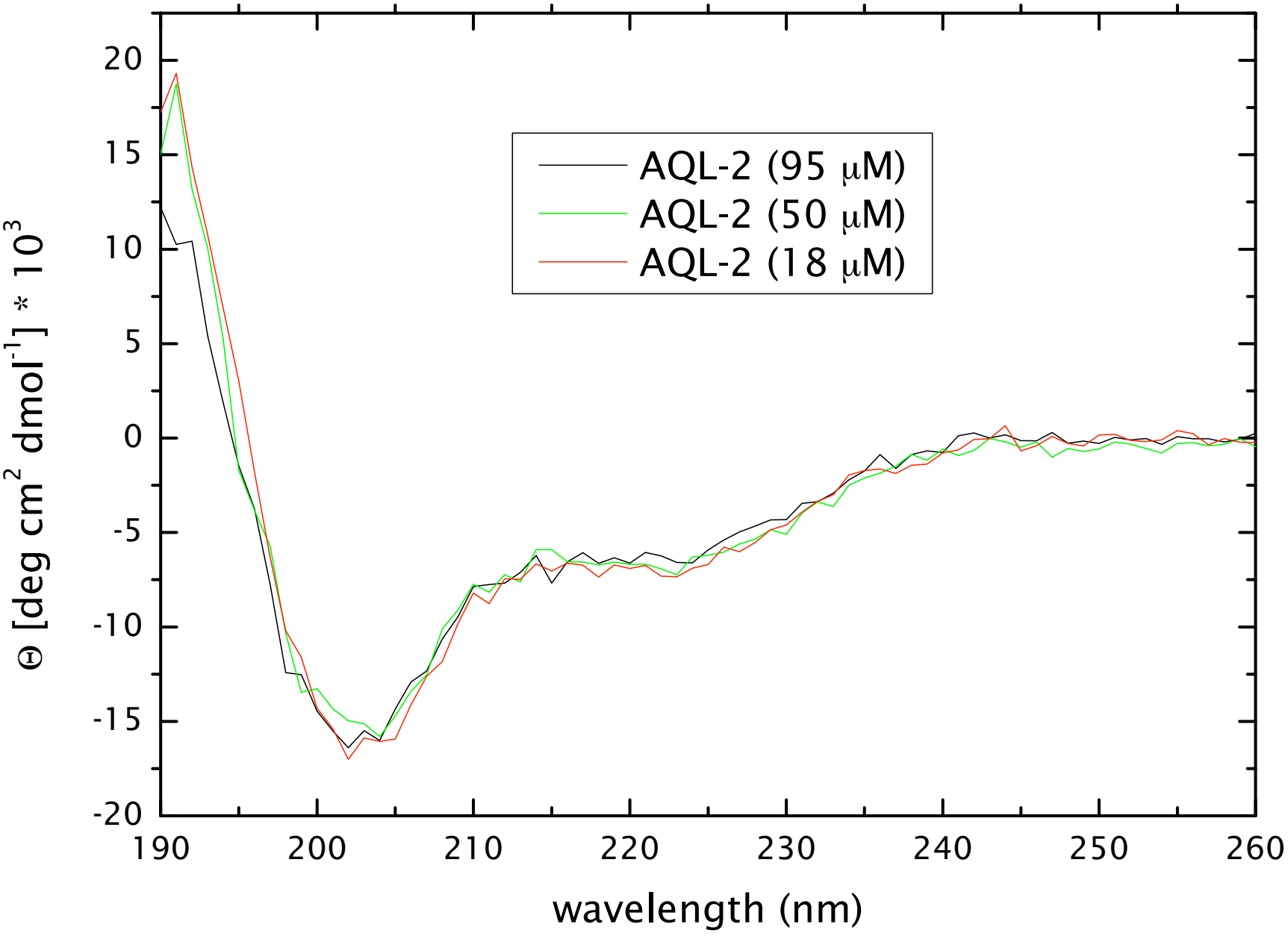
AQL-2 (95 μM)
AQL-2 (50 μM)
AQL-2 (18 μM)
Θ [deg cm^2 dmol^{-1}] * 10^3
wavelength (nm)
20
15
10
5
0
-5
-10
-15
-20
190
200
210
220
230
240
250
260

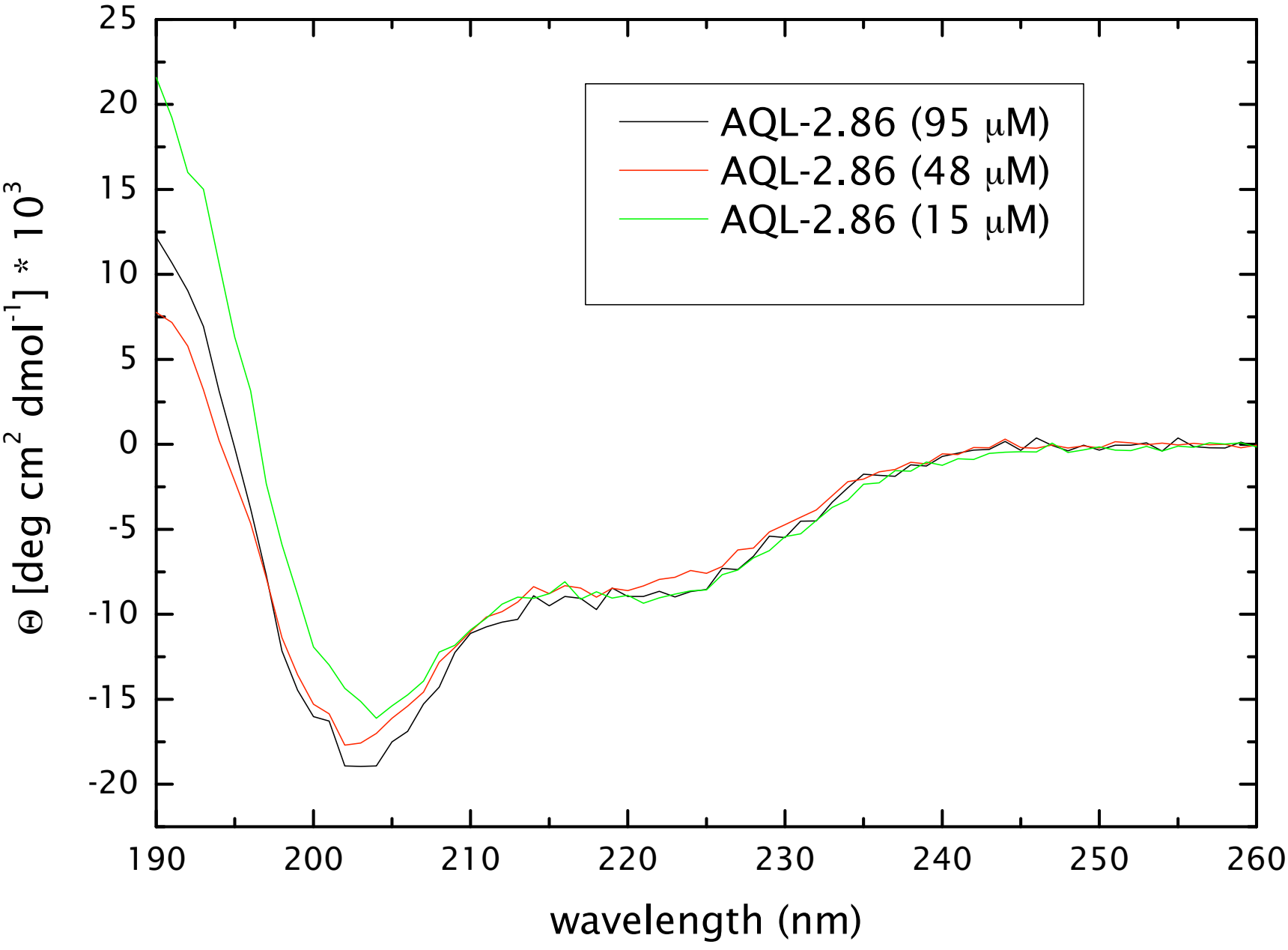
AQL-2.86 (95 μM)
AQL-2.86 (48 μM)
AQL-2.86 (15 μM)
Θ [deg cm2 dmol-1] * 10^3
wavelength (nm)
25
20
15
10
5
0
-5
-10
-15
-20
190
200
210
220
230
240
250
260

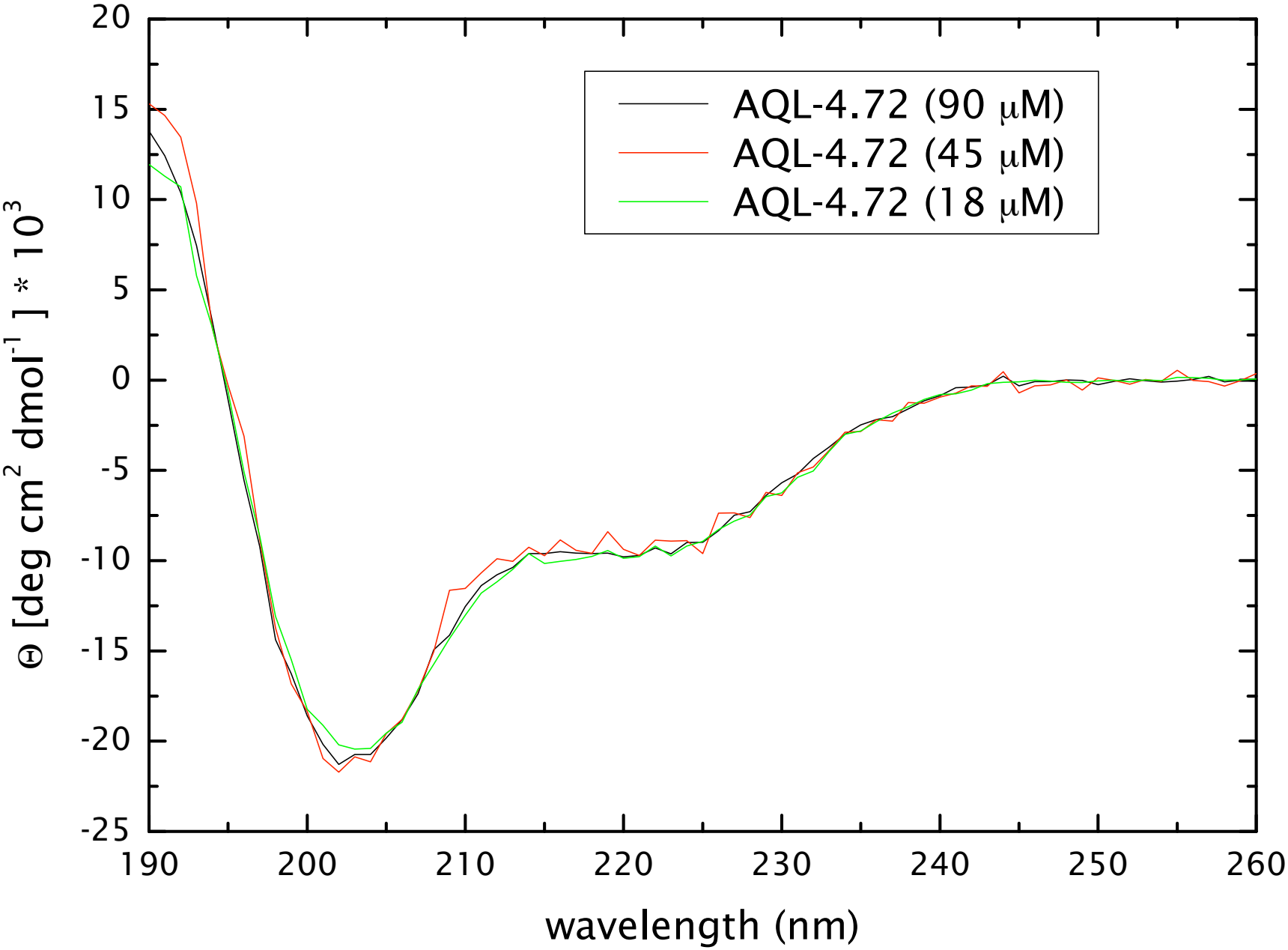
AQL-4.72 (90 μM)
AQL-4.72 (45 μM)
AQL-4.72 (18 μM)
Θ [deg cm2 dmol-1] * 10^3
wavelength (nm)
20
15
10
5
0
-5
-10
-15
-20
-25
190
200
210
220
230
240
250
260

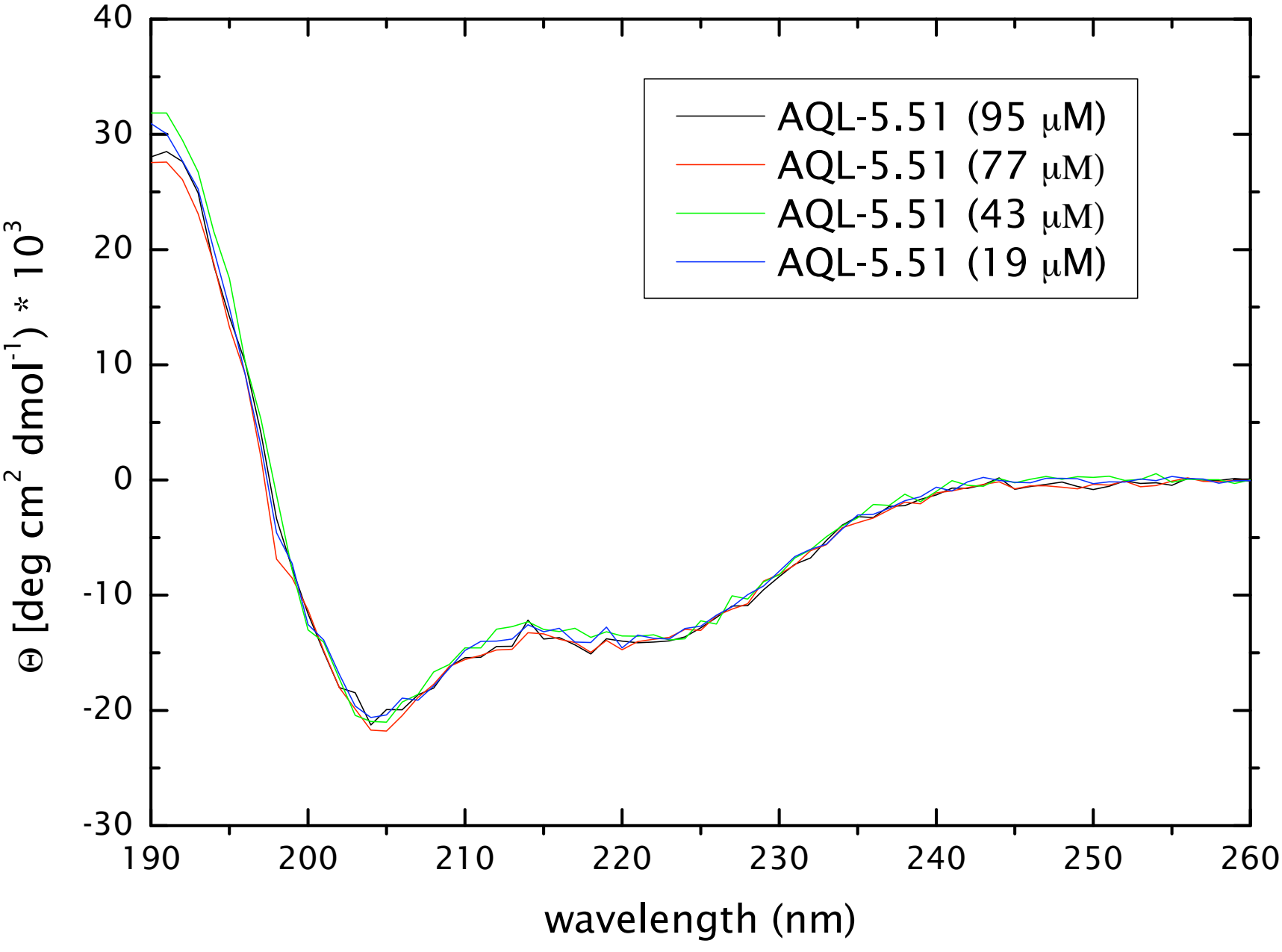
AQL-5.51 (95 μM)
AQL-5.51 (77 μM)
AQL-5.51 (43 μM)
AQL-5.51 (19 μM)
Θ [deg cm2 dmol-1) * 10^3
wavelength (nm)
40
30
20
10
0
-10
-20
-30
190
200
210
220
230
240
250
260

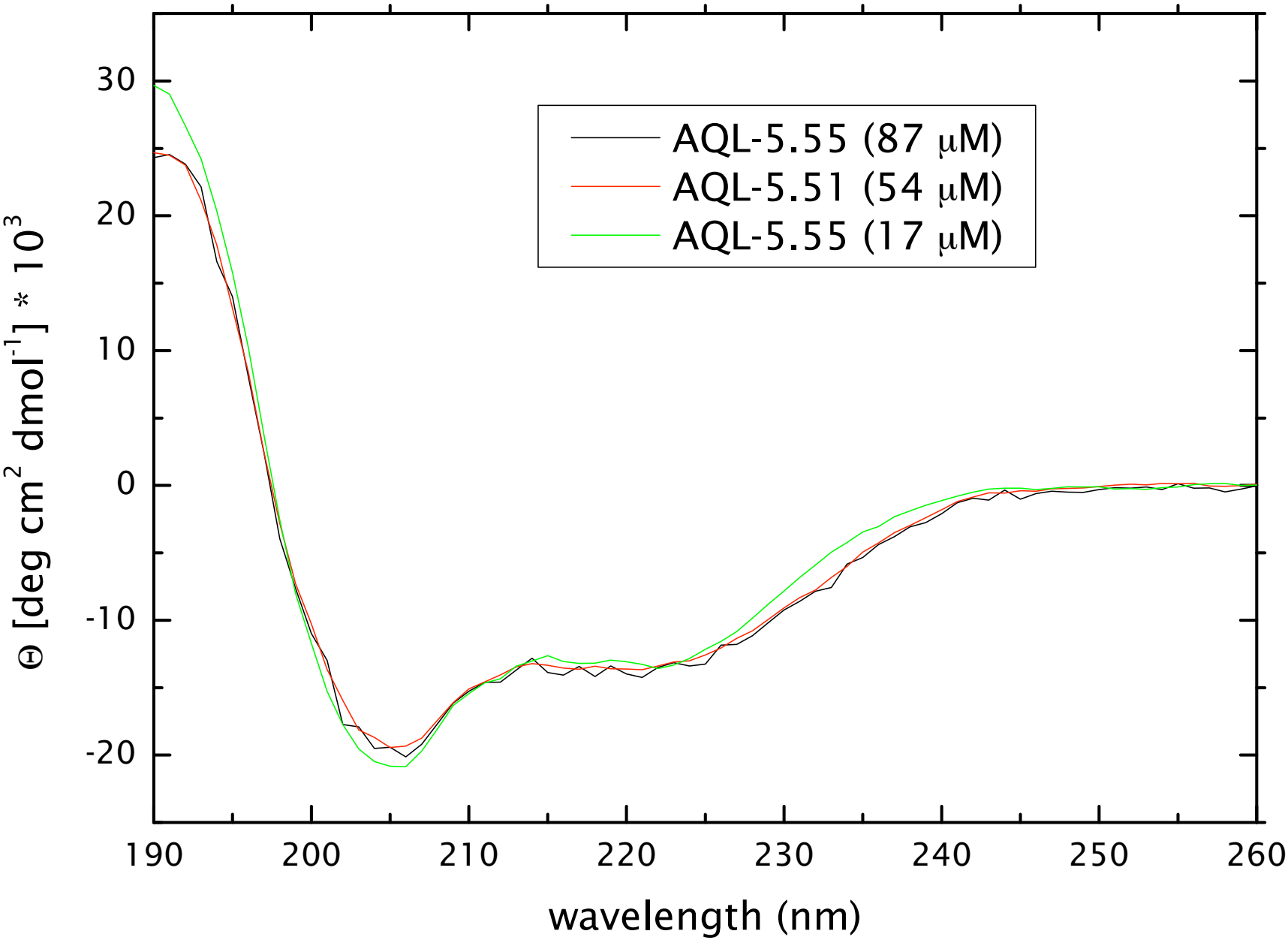
AQL-5.55 (87 μM)
AQL-5.51 (54 μM)
AQL-5.55 (17 μM)
Θ [deg cm^2 dmol^{-1}] * 10^3
30
20
10
0
-10
-20
190
200
210
220
230
240
250
260
wavelength (nm)

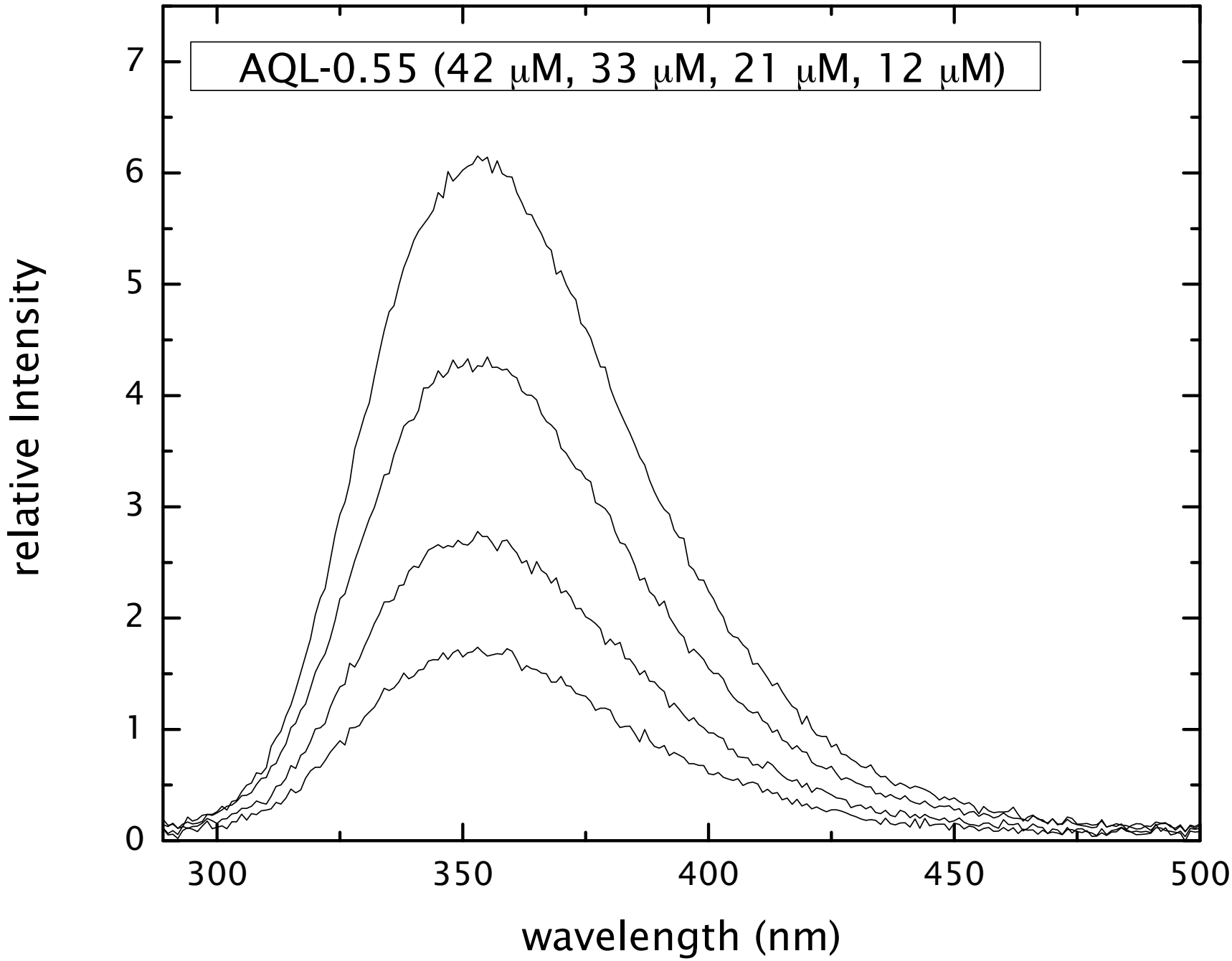
AQL-0.55 (42 μM, 33 μM, 21 μM, 12 μM)
relative Intensity
wavelength (nm)
0
1
2
3
4
5
6
7
300
350
400
450
500

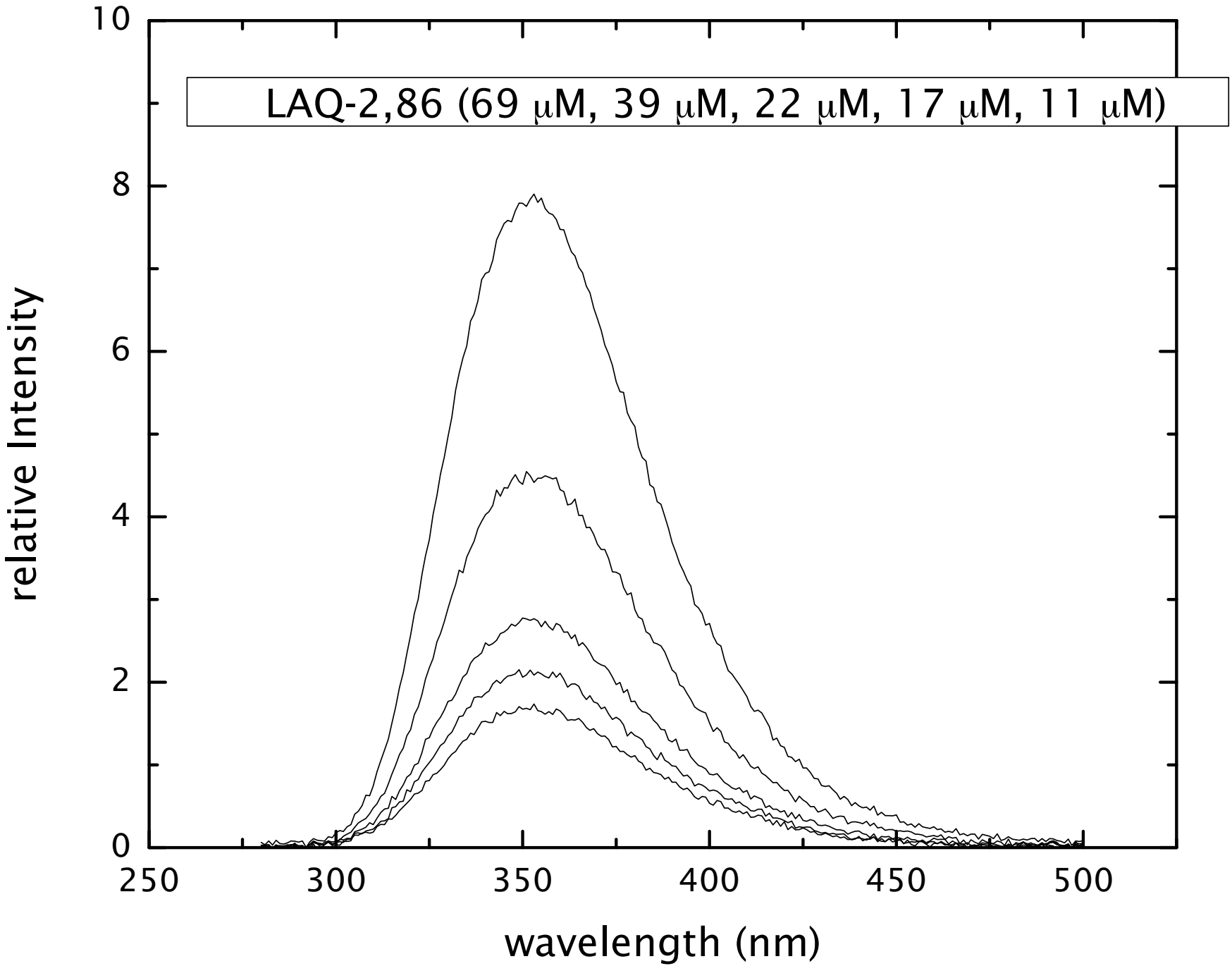
LAQ-2,86 (69 μM, 39 μM, 22 μM, 17 μM, 11 μM)
relative Intensity
wavelength (nm)
0
2
4
6
8
10
250
300
350
400
450
500

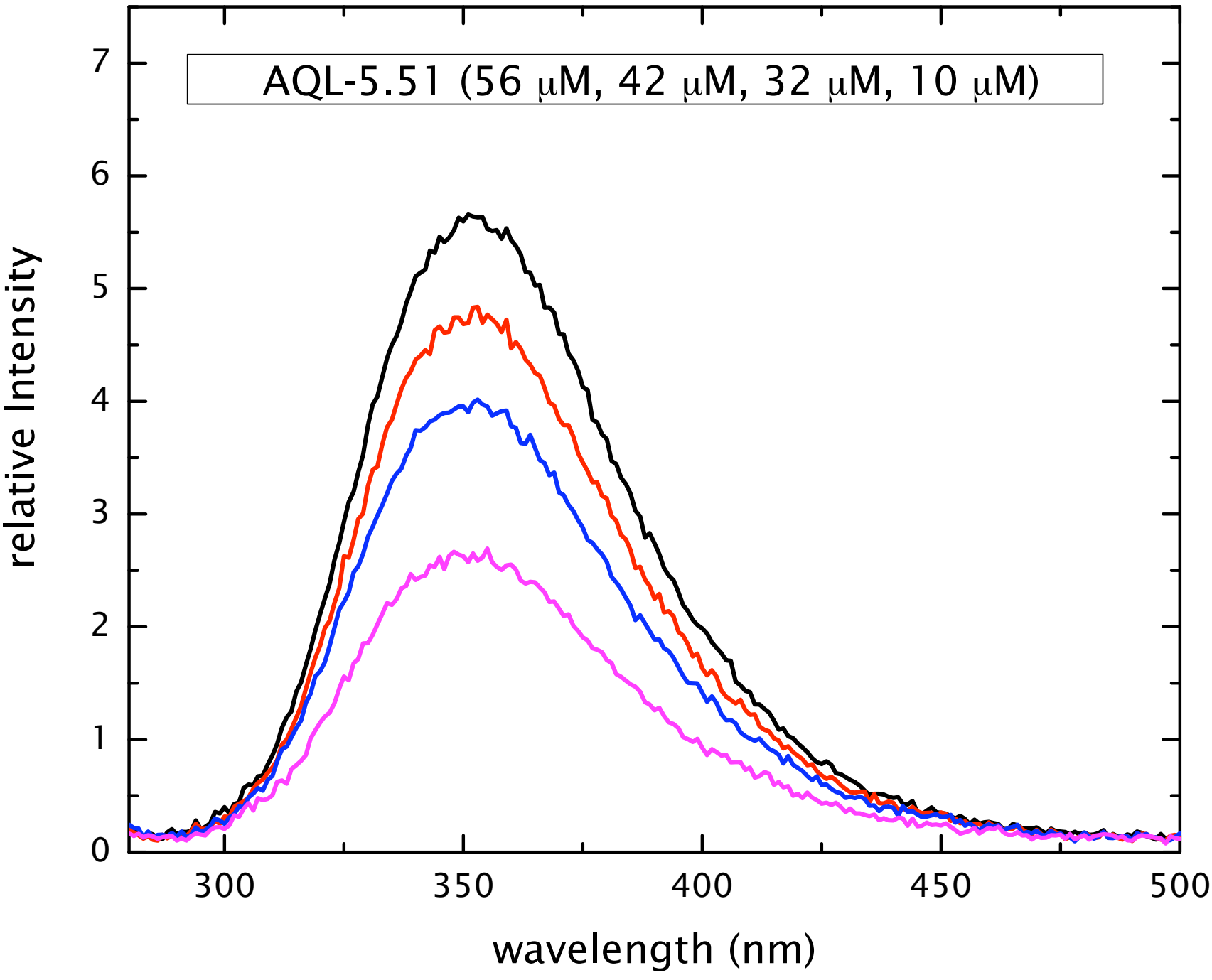
AQL-5.51 (56 μM, 42 μM, 32 μM, 10 μM)
relative Intensity
0
1
2
3
4
5
6
7
300
350
400
450
500
wavelength (nm)

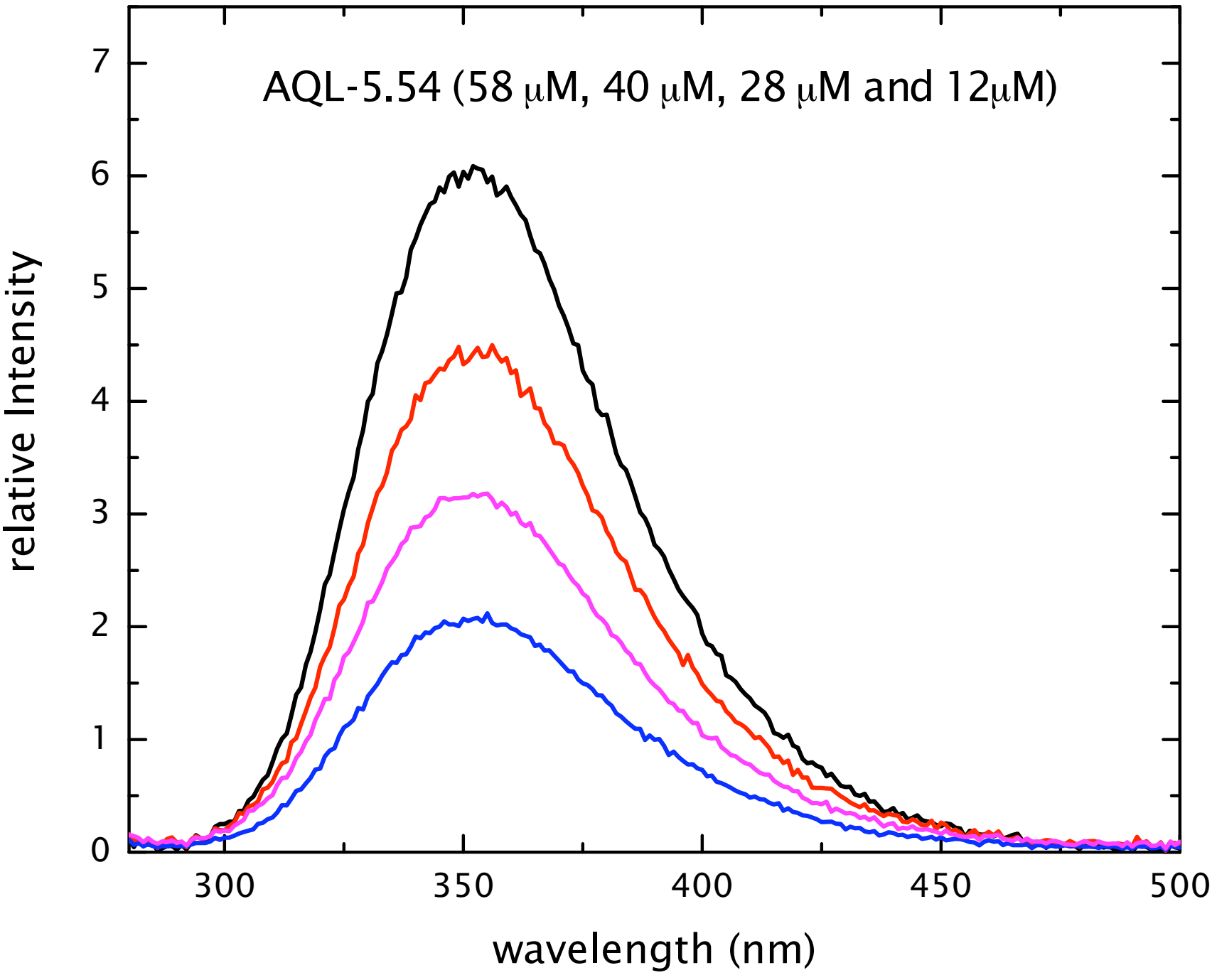
AQL-5.54 (58 μM, 40 μM, 28 μM and 12μM)
relative Intensity
0
1
2
3
4
5
6
7
300
350
400
450
500
wavelength (nm)